

GST report for GSTBest_condensed

October 20, 2015

1 Overview

This report presents a gate-set tomography (GST) analysis of a dataset called “GSTBest_condensed”.

GST characterizes logic operations on a quantum device (e.g., a qubit), by treating it as a black box. This black box is equipped with a small set of “buttons” that apply quantum *gates* to the quantum system inside. One button initializes it, a second button triggers a 2-outcome measurement, and the remaining buttons perform transformations. We avoid assumptions about the device’s operation whenever possible. Currently, we assume that:

- the quantum device is a qubit (has a Hilbert space of dimension 2),
- each *gate*, or logic operation, can be represented by a stationary Markov process (a.k.a. “quantum channel”).

The core of GST is an algorithm that takes certain inputs, and produces certain outputs. The *input* to GST comprises (1) a list of data, and (2) “target” gateset describing the *ideal* behavior of the device. GST data comprises a list of experiments – each described by the sequence of gates that was applied – and, for each experiment, two integer *counts* stating how often the “plus” and “minus” results were observed. The target gates are used *only* to (a) report how consistent the estimates are with the target, and (b) choose the best *gauge* in which to report the results. GST does not take them into account in its core analysis, and there is no possibility of circularity or other “cheating”.

GST’s primary output is an estimated *gateset* that models or fits the device’s observed behavior. Gatesets are of the form $\{\rho_0, E_0, \{G_k\}\}$, where

- ρ_0 is an estimate of the density matrix in which the device gets initialized,
- $\{E_0, \mathbb{I} - E_0\}$ is an estimate of the POVM describing how it gets measured,
- and each of the G_k is an estimate of the superoperator (quantum process) describing the corresponding gate.

Unless something went wrong (usually it doesn’t), the output of GST is the best possible fit to the data. This should also mean that they are a very accurate description of what happens when you trigger a gate on your device. However, this happy conclusion relies on two assumptions:

1. The experiments were chosen wisely, so that the only gate sets consistent with their results are very close to the true behavior. This is usually true. The main failure mode occurs when you were not able to perform *long* sequences (e.g., because your decoherence rate is very high), in which case accuracy may be limited.
2. The operations you are performing really are stationary (time-independent), Markovian, and acting on a quantum system with the correct Hilbert space dimension. These assumptions define the *model* that GST fits to the data. **They are usually not true!** Quantum operations are usually at least a little bit non-Markovian. In this report (Section 4) we provide extensive self-checks to identify and diagnose violations of the model. If your system *is* visibly non-Markovian, then (a) these checks will probably warn you of it, and (b) the other quantities reported here should be treated with caution – using GST on non-Markovian gates violates the warranty!

This document is organized into three main sections, which address three broad questions.

- Section 2: What inputs did you give GST?
- Section 3: What estimate did GST output, and what does it mean?
- Section 4: How reliable are the results? (How badly was the model violated?)

Section 2 is primarily useful to verify that the inputs were correct. Section 3 is the most important: it presents the raw estimates derived by the GST algorithm, and also provides a variety of derived quantities that may be useful in interpreting what this estimate means.

Section 4) is dedicated to summarizing how well the model imposed by GST was able to fit the data, relative to what is expected of a “good” model. This is *not* related to “How close is the GST estimate to the target gates?”, which is addressed in Section 3. It is also not the same as “How large are the error bars on the GST estimate?”, which is a good question that we do not directly address at this time. Instead, Section 4 is intended to tell you whether (a) you should take the GST estimate at face value, or (b) it should be treated skeptically because *no* gate set was capable of fitting the data.

Finally, appendices may be present (depending on which options were chosen when this report was generated). Appendices present more detailed debugging information, elaborating on the goodness-of-fit metrics presented in Section 4.

2 Input Summary

The input for this GST analysis comprised: (1) a target gateset (see Tables 1-2); and (2) a dataset called “GSTBest_condensed”.

2.1 Target Gateset

The target gateset describes the ideal initial state (density matrix), measurement (POVM effect), and gate operations (superoperators). Typically, density matrices and POVM effects are represented as square $d \times d$ matrices on a Hilbert space \mathcal{H} . In GST, it is often more convenient to represent them as d^2 -element vectors in the Hilbert-Schmidt space $\mathcal{B}(\mathcal{H})$ of linear operators on \mathcal{H} . Both representations are shown in Table 2. Superoperators are sometimes represented in Choi or Kraus form, but for GST it is more convenient to represent them as square $d^2 \times d^2$ matrices that multiply associatively and act on $\mathcal{B}(\mathcal{H})$. These are shown in Table 2.

These Hilbert-Schmidt space representations require choosing a basis $\{M_i\}$ for $\mathcal{B}(\mathcal{H})$. We use the *Pauli basis*, comprising the four 2×2 Pauli matrices (including the identity $\mathbb{1}$) for $d = 2$. In $d > 2$, we use the analogous Gell-Mann matrices as a basis. The choice of this basis is what is meant when state preparations and measurements are written as vectors and gate operations are written as matrices in the “Pauli basis”. Keep in mind that we want to use an orthonormal basis, so the basis matrices are normalized so that $\langle M_i | M_j \rangle = \text{Tr} M_i^\dagger M_j = \delta_{ij}$. In $d = 2$, this means that the basis matrices are $M_i = \frac{1}{\sqrt{2}}\sigma_i$.

The ideal SPAM operations for your particular case are given in Table 1. The ideal *logic gate* operations are given, as superoperators written in the Pauli basis, in Table 2.

In most cases, the ideal/target logic gates are reversible unitary rotations. The corresponding superoperators are orthogonal rotations on $\mathcal{B}(\mathcal{H})$. For your convenience, Table 2 also lists (for each logic gate) an axis of rotation [as a vector in $\mathcal{B}(\mathcal{H})$] and an angle of rotation.

2.2 GST Input Data

The most important input to GST is a *dataset* – a list of experimental counts or frequencies, each associated with a *gate sequences*. Gate sequences are also referred to as “gate strings”. Each gate sequence defines an experiment, in which you (1) initialize the device, (2) apply the operations specified by the gate sequence, and (3) measure and record the result (“plus” or “minus”).

Typically, the gate sequences that appear in the dataset are generated by the following process:

1. A small set of short gate sequences called *germs* are chosen,

Operator	Hilbert-Schmidt vector (Pauli basis)	Matrix
ρ_0	0.7071	$\begin{pmatrix} 1 & 0 \\ 0 & 0 \end{pmatrix}$
	0	
	0	
	0.7071	
E_0	0.7071	$\begin{pmatrix} 0 & 0 \\ 0 & 1 \end{pmatrix}$
	0	
	0	
	-0.7071	

Table 1: **Target gateset: SPAM (state preparation and measurement) gates.** These are the *ideal* input state (ρ_0) and ‘plus’ POVM effect E_0 for the device on which we report. SPAM gates are given here both as $d \times d$ matrices, and in “vectorized” form as d^2 -dimensional vectors in $\mathcal{B}(\mathcal{H})$. See Table 5 for GST estimates of the actual ρ_0 and E_0 implemented in this experiment.

Gate	Superoperator (Pauli basis)	Rotation axis	Angle
Gi	$\begin{pmatrix} 1 & 0 & 0 & 0 \\ 0 & 1 & 0 & 0 \\ 0 & 0 & 1 & 0 \\ 0 & 0 & 0 & 1 \end{pmatrix}$	0	0π
		1	
		0	
		0	
Gx	$\begin{pmatrix} 1 & 0 & 0 & 0 \\ 0 & 1 & 0 & 0 \\ 0 & 0 & 0 & -1 \\ 0 & 0 & 1 & 0 \end{pmatrix}$	0	0.5π
		1	
		0	
		0	
Gy	$\begin{pmatrix} 1 & 0 & 0 & 0 \\ 0 & 0 & 0 & 1 \\ 0 & 0 & 1 & 0 \\ 0 & -1 & 0 & 0 \end{pmatrix}$	0	0.5π
		0	
		1	
		0	

Table 2: **Target gateset: logic gates.** These are the *ideal* (generally unitary) logic gates. Each has a name starting with “G”, and is represented as a $d^2 \times d^2$ *superoperator* that acts by matrix multiplication on vectors in $\mathcal{B}(\mathcal{H})$. For each gate, its axis of rotation (in $\mathcal{B}(\mathcal{H})$) and angle of rotation are also given. See Table 7 for GST estimates of the actual logic gates implemented in this experiment.

2. A small set of short *fiducial sequences* are chosen so that, when applied to ρ_0 or E_0 , they generate an informationally complete set of states or effects.
3. Each germ is concatenated with itself to form *base sequences* of length approximately $1, 2, 4, 8, \dots L_{max}$.
4. Each base sequence is sandwiched between every possible pair of fiducial sequences.

The dataset comprises all sandwiched base sequences. A few other short sequences (e.g., those corresponding to the empty base sequence) may also appear.

The fiducial sequences and germs for *this* dataset are given in Table 3. An overview of the information contained in the file you provided for dataset “GSTBest_condensed” is given in Table 4.

This table also contains one derived quantity, the spectrum of the largest *Gram matrix* that GST could extract from the data. This is included here rather than in the analysis because it is not useful for predictive purposes, and therefore is not part of the estimate. It serves, instead, to tell you something about the quality of the data. More precisely, it tells you about the dimension of the state space that is explored by the fiducial sequences. This should be d^2 -dimensional [because the fiducials are intended to explore all of $\mathcal{B}(\mathcal{H})$], and therefore the spectrum listed in Table 4 should (ideally) have exactly d^2 elements that are large and nonzero. In practice, you should see d^2 large elements, and a rapid drop in magnitude thereafter. If fewer than d^2 elements are large, then the fiducials were poorly chosen and are not exploring the state space effectively. If

more than d^2 are large, then the system is experiencing strong non-Markovian effects (e.g., strong coupling to environmental degrees of freedom) or it has a larger Hilbert space dimension than expected.

#	Prep.	Measure
1		
2	Gx	Gx
3	Gy	Gy
4	Gx · Gx	Gx · Gx
5	Gx · Gx · Gx	Gx · Gx · Gx
6	Gy · Gy · Gy	Gy · Gy · Gy

#	Germ
1	Gx
2	Gy
3	Gi
4	Gx · Gy
5	Gx · Gy · Gi
6	Gx · Gi · Gy
7	Gx · Gi · Gi
8	Gy · Gi · Gi
9	Gx · Gx · Gi · Gy
10	Gx · Gy · Gy · Gi
11	Gx · Gx · Gy · Gx · Gy · Gy

Table 3: **Fiducial sequences and germs.** See discussion in text.

Quantity	Value
Number of strings	4273
Gate labels	Gx, Gy, Gi
SPAM labels	plus, minus
	0.0182
	0.1548
	0.2594
Gram singular vals	0.9421
	1.0148
	1.467
	3.4495

Table 4: **General dataset properties.** See discussion in text.

3 Output from GST

The primary output of GST is an estimated gateset. This section presents the raw estimate, and then some useful derived quantities of the estimated gates, including comparisons to the target gates.

3.1 Raw GST estimates

Table 5 reports the estimated SPAM operations, and Table 7 reports the logic gate operations. The estimated SPAM gates (ρ_0 and E_0) are vectors in $\mathcal{B}(\mathcal{H})$, and the estimated logic gates are superoperators represented as matrices acting on $\mathcal{B}(\mathcal{H})$, all in the Pauli basis. By taking the dot product of state preparation and measurement vectors estimated SPAM probabilites are computed in Table 6. Tables 5 and 7 report 95% confidence intervals for each of the gate matrix and SPAM vector elements. A confidence region is obtained by approximating the log-likelihood (see below) as being quadratic about its minimum, and determining the ellipsoid where this approximation equals a value, C , defined below. For a given parameter (e.g. gate or SPAM vector element) x , a confidence interval is obtained by projecting the ellipsoidal region onto that x 's axis. This computes a 1-dimensional 95% confidence interval for the profile log-liklihood for x , and for this reason the value of C used above is chosen such that $\text{CDF}[\chi_1^2](C) = 95\%$ (that is, at the value C the cumulative density function of a χ_1^2 distribution reaches 95%). If, instead, the interval corresponding to a projection of the 95% multi-dimensional confidence region (defined by C s.t. $\text{CDF}[\chi_n^2](C) = 95\%$,

where $n = 31$ is the number of non-gauge gate set parameters) is desired, then the all the interval widths reported here should be multiplied by 3.42. The resulting confidence interval is always symmetric about the estimated value, and we report the half-width of the intervals in the tables. In table 6 and those in the following section, we specify the 95% confidence intervals of derived quantities in using *value \pm half-width* notation. The derived-quantity confidence intervals in section 3.2 are computed by finding the minimum and maximum values of the linearization of the derived quantity (e.g. fidelity).

Operator	Hilbert-Schmidt vector (Pauli basis)	95% C.I. 1/2-width	Matrix
ρ_0	0.7071	0	
	0.0065	0.0088	$\begin{pmatrix} 0.9894 & 0.0056e^{i0.6} \\ 0.0056e^{-i0.6} & 0.0106 \end{pmatrix}$
	-0.0045	0.0094	
	0.6921	0.0009	
ρ_0	0.701	0.0019	
	-0.0008	0.0088	$\begin{pmatrix} -0.0064 & 0.0006e^{i2.8} \\ 0.0006e^{-i2.8} & 0.9978 \end{pmatrix}$
	-0.0003	0.0097	
	-0.7101	0.0012	

Table 5: **The GST estimate of the SPAM operations.** Compare to Table 1.

	E_0	E_{-1}
ρ_0	0.004272	0.995728
	± 0.001578	± 0.001578

Table 6: **GST estimate of SPAM probabilities.** Computed by taking the dot products of vectors in Table 5.

Gate	Superoperator (Pauli basis)	95% C.I. 1/2-width
G_i	$\begin{pmatrix} 1 & 0 & 0 & 0 \\ -4 \times 10^{-6} & 1 & -5 \times 10^{-5} & -4 \times 10^{-5} \\ -2 \times 10^{-5} & 0.0001 & 0.9999 & 3 \times 10^{-6} \\ 2 \times 10^{-5} & -3 \times 10^{-5} & -8 \times 10^{-8} & 1 \end{pmatrix}$	$\begin{pmatrix} 0 & 0 & 0 & 0 \\ 2 \times 10^{-5} & 2 \times 10^{-5} & 0.0001 & 0.0001 \\ 2 \times 10^{-5} & 0.0001 & 3 \times 10^{-5} & 0.0001 \\ 2 \times 10^{-5} & 0.0001 & 0.0001 & 2 \times 10^{-5} \end{pmatrix}$
G_x	$\begin{pmatrix} 1 & 0 & 0 & 0 \\ -2 \times 10^{-5} & 0.9999 & 7 \times 10^{-7} & -2 \times 10^{-5} \\ 8 \times 10^{-6} & 2 \times 10^{-5} & 0.0001 & -0.9999 \\ 8 \times 10^{-6} & 1 \times 10^{-5} & 0.9999 & 0.0001 \end{pmatrix}$	$\begin{pmatrix} 0 & 0 & 0 & 0 \\ 2 \times 10^{-5} & 3 \times 10^{-5} & 0.0001 & 0.0001 \\ 2 \times 10^{-5} & 0.0001 & 0.0001 & 3 \times 10^{-5} \\ 2 \times 10^{-5} & 0.0001 & 3 \times 10^{-5} & 0.0001 \end{pmatrix}$
G_y	$\begin{pmatrix} 1 & 0 & 0 & 0 \\ 7 \times 10^{-6} & 2 \times 10^{-5} & 1 \times 10^{-6} & 0.9999 \\ 8 \times 10^{-7} & 2 \times 10^{-5} & 1 & 1 \times 10^{-5} \\ -8 \times 10^{-6} & -0.9999 & -2 \times 10^{-5} & -7 \times 10^{-7} \end{pmatrix}$	$\begin{pmatrix} 0 & 0 & 0 & 0 \\ 2 \times 10^{-5} & 0.0001 & 0.0001 & 3 \times 10^{-5} \\ 2 \times 10^{-5} & 0.0001 & 2 \times 10^{-5} & 0.0001 \\ 2 \times 10^{-5} & 2 \times 10^{-5} & 0.0001 & 0.0001 \end{pmatrix}$

Table 7: **The GST estimate of the logic gate operations.** Compare to Table 2.

The estimated gates can be compared directly to the target gateset given in Section 2. Ideally, they would match. In practice, of course, they won't. One of the best ways we have found to evaluate the significance of discrepancies is to compare *derived* quantities – i.e., certain properties calculated from the gate matrices and SPAM vectors. Deriving quantities from these raw outputs occupies the remainder of this section.

3.2 Derived quantities

Generally, the first thing that you want to know is “How far from ideal are the gates?” To answer this, this report tabulates several well-known metrics of distance. Table 8 lists the discrepancy from each estimated

gate to its corresponding target, as measured by:

1. **Process infidelity.** Infidelity is simply $1 - F$, where F is a *fidelity*. The process fidelity between quantum processes G_a and G_b is given by $F = \text{Tr} \left(\sqrt{\sqrt{(\chi_a)\chi_b}\sqrt{(\chi_a)}} \right)^2$, where χ_a and χ_b are the Jamiolkowski states (normalized Choi process matrices) corresponding to gate matrices G_a and G_b respectively. If the target is unitary (as is often the case), $F = \text{Tr}(\chi_a\chi_b)$. Process infidelity is roughly what is measured in randomized benchmarking protocols; it quantifies the *incoherent* error rate if coherent errors (e.g. over rotations) are not allowed to accumulate.
2. **Trace distance.** This is the *Jamiolkowski trace distance* between the Jamiolkowski states corresponding to the two processes: $d_{tr} = |\chi_a - \chi_b|_1 = \text{Tr} \left(\sqrt{(\chi_a - \chi_b)^2} \right)$. This distance is useful primarily as a proxy for the *diamond norm distance*, because $d_{tr} \leq d_\diamond \leq \dim(\mathcal{H})d_{tr}$. The diamond norm distance is an upper bound on the rate of error under any possible circumstance (including coherent accumulation of errors) and is often used in proofs of fault tolerance. For gates dominated by coherent/unitary error, it is common to see $d_\diamond \approx \sqrt{1 - F}$. For gates dominated by incoherent error, $d_\diamond \approx 1 - F$.
3. **Diamond Norm.** The diamond norm between two quantum processes G_a and G_b is given by $\|G_a - G_b\|_\diamond = \sup_\rho \| (G_a \otimes I_k)(\rho) - (G_b \otimes I_k)(\rho) \|_1$, where I_k is the k -dimensional identity operation, $\|\cdot\|_1$ denotes the trace norm, and the supremum is taken over all $k \geq 1$ and density matrices ρ of dimension nk , with n the dimension of G_a and G_b . The diamond norm is also called the *completely bounded trace norm*, and plays the analogous role for quantum process distinguishability that the trace norm plays for density matrices. Specifically, the optimal probability of distinguishing G_a from G_b after a *single evaluation* is given by $\frac{1}{2} + \frac{1}{4} \|G_a - G_b\|_\diamond$.
4. **Frobenius-norm distance.** The Frobenius norm distance between two gates G_a and G_b is simply $d_F = \sqrt{\text{Tr} \left[(G_a - G_b)^2 \right]}$. It has no known *operational* interpretation, but is very convenient as a rough measure of inaccuracy. It is also equal to the sum of the RMS errors in the individual matrix elements of the gates.

It's also useful to know *how* the real gates (or, more precisely, GST's estimates of the real gates) differ from the targets. There are several ways we could represent this, but the most useful involves an *error generator*. These are also given in Table 8. The final column of the table lists, for each gate, a Lindbladian superoperator \mathbb{L} . It is defined by the equation $\hat{G} = G_{\text{target}} e^{\mathbb{L}}$, where \hat{G} is the estimate and G_{target} is the ideal gate. This Lindbladian would be zero if the gates were perfect, and its overall magnitude is approximately equal to the diamond distance (or Jamiolkowski trace distance) between the target gate and the estimate.

It's usually useful to understand *how* gates fail. The error generators in Table 8 provide one view on this, but they are not necessarily intuitive. For example, you might want to know whether your gate suffers depolarizing, dephasing, or over-rotation errors. In Table 9, the estimated gates are decomposed into: (1) rotations (including angle and axis errors); (2) incoherent *diagonal* decay rates (depolarizing or T_1 noise); and (3) incoherent *off-diagonal* decay rates (dephasing or T_2 noise). These analyses can be compared with a the similar decomposition of the target gates (cf. table 2). Note that for some erroneous gates, this decomposition simply fails; if the numbers make no sense, this is probably the case.

It might be useful to know the closest *unitary* operation to the estimated gate, and how close it is. Usually, you were trying to implement a unitary. If the closest unitary to G was indeed G_{target} , then all errors are incoherent; if not, you might be able to tweak the gate parameters to get closer relatively easily. Also, implementing a particular unitary may be less important than just achieving *some* set of mutually independent unitaries. In these and other cases, the distance from an estimated gate to its closest unitary approximation is of interest.

Table 10 lists, for each estimated gate, the properties of its closest unitary approximation. The table defines the closest unitary, in terms of an axis and angle (in $\mathcal{B}(\mathcal{H})$) of rotation. It also presents the process fidelity and Jamiolkowski trace distance between the estimated gate and its closest unitary approximation. A sanity check is computed by comparing the fidelity of the obtained closest unitary with a theoretical upper bound (if a value greater than one appears in this column then the other values in that row may be

Gate	Process Infidelity	$1/2$ -width Trace Distance	$1/2$ -width \diamond -Norm	Frobenius Distance
Gi	0.000041	0.000052	0.00006	0.000136
	± 0.00001	± 0.000015	± 0.000024	± 0.000039
Gx	0.000054	0.000079	0.00008	0.000195
	± 0.000014	± 0.000024	± 0.000023	± 0.00006
Gy	0.000069	0.000069	0.00007	0.000176
	± 0.000013	± 0.000013	± 0.000013	± 0.000035

Gate	Error Generator
Gi	$\begin{pmatrix} 0 & 0 & 0 & 0 \\ -4 \times 10^{-6} & -5 \times 10^{-5} & -5 \times 10^{-5} & -4 \times 10^{-5} \\ -2 \times 10^{-5} & 0.0001 & -0.0001 & 3 \times 10^{-6} \\ 2 \times 10^{-5} & -3 \times 10^{-5} & -8 \times 10^{-8} & -4 \times 10^{-5} \end{pmatrix}$
Gx	$\begin{pmatrix} 0 & 0 & 0 & 0 \\ -2 \times 10^{-5} & -0.0001 & 7 \times 10^{-7} & -2 \times 10^{-5} \\ 8 \times 10^{-6} & 1 \times 10^{-5} & -0.0001 & 0.0001 \\ -8 \times 10^{-6} & -2 \times 10^{-5} & -0.0001 & -0.0001 \end{pmatrix}$
Gy	$\begin{pmatrix} 0 & 0 & 0 & 0 \\ 8 \times 10^{-6} & -0.0001 & 2 \times 10^{-5} & 7 \times 10^{-7} \\ 8 \times 10^{-7} & 2 \times 10^{-5} & -4 \times 10^{-5} & 1 \times 10^{-5} \\ 7 \times 10^{-6} & 2 \times 10^{-5} & 1 \times 10^{-6} & -0.0001 \end{pmatrix}$

Table 8: **Comparison of GST estimated gates to target gates.** This table presents, for each of the gates, three different measures of distance or discrepancy from the GST estimate to the ideal target operation. See text for more detail. The second table lists the “Error Generator” for each gate, which is the Lindbladian \mathbb{L} that describes *how* the gate is failing to match the target. This error generator is defined by the equation $\hat{G} = G_{\text{target}} e^{\mathbb{L}}$.

inaccurate). If these numbers are similar to those in Table 8, then the gates are as close to the targets as they are to *any* unitary.

Finally, Table 11 presents each estimated gate’s *Choi matrix*, along with its spectrum. The Choi matrix (sometimes ambiguously referred to as the “process matrix”) is an alternative way to describe a process. We usually prefer the “superoperator representation”, which has the very useful property that the process matrix corresponding to applying G_a and then G_b is simply $G_b G_a$. This is completely false for the Choi representation. Nonetheless, the Choi representation is often useful, so we present it here – but without a detailed discussion of its properties (see, e.g. the textbook by Nielsen and Chuang).

The Choi matrix $\chi(G)$ for a gate G can be simply understood in either of two ways. First, it is equivalent (up to choice of basis) to the *Jamiolkowski state* defined by applying G to one half of a maximally entangled bipartite state. Second, it is the general (non-diagonal) form of the well-known Kraus representation, $G[\rho] = \sum_i K_i \rho K_i^\dagger$. The Choi matrix behaves in many ways like a quantum state, and appears naturally in expressions for the process fidelity and Jamiolkowski trace distance just as density matrices would enter these expressions when computing differences between states.

Additionally, the condition of *complete positivity* or CP (which all real quantum processes must satisfy) is simply the positivity of the Choi matrix. Thus, negative eigenvalues in Table 11 indicate that the estimate violates complete positivity. If they are very small, they may simply indicate statistical fluctuations (unitary gates have χ matrices with zero eigenvalues, so any small fluctuation is likely to violate CP). If they are large, they serve as a warning that (1) the model of CPTP maps is probably violated (usually because of non-Markovian behavior), and (2) this estimate may produce negative or greater-than-unity probabilities. GST does *not* generally impose complete positivity (although it is an option), precisely because violation of CP is a warning flag for non-Markovian behavior (which is very common in experimental qubits).

Gate	Eigenvalues		Fixed pt	Rotn. axis	Diag. decay	Off-diag. decay
Gi	1	5×10^{-5}	1	0		
	$0.9999e^{i0.0}$	$\pm 0.0001e^{i0.9}$	0	0.4704	0.000018	0.000073
	$0.9999e^{-i0.0}$	$\pm 0.0001e^{i0.9}$	0	0.384	± 0.000048	± 0.00003
	1	0	0	-0.7945		
Gx	$0.9999e^{i1.6}$	$0.0001e^{i0.4}$	1	0		
	$0.9999e^{-i1.6}$	$\pm 0.0001e^{i0.4}$	0	-1	0.000056	0.00008
	0.9999	$\pm 3 \times 10^{-5}$	2×10^{-7}	-3×10^{-6}	± 0.000026	± 0.000026
	1	0	8×10^{-6}	-1×10^{-5}		
Gy	$0.9999e^{i1.6}$	$0.0001e^{i0.4}$	1	0		
	$0.9999e^{-i1.6}$	$\pm 0.0001e^{i0.4}$	-2×10^{-7}	-1×10^{-5}	0.000039	0.000118
	1	$\pm 2 \times 10^{-5}$	0	1	± 0.000023	± 0.000024
	1	0	-7×10^{-6}	-1×10^{-5}		

Gate	Angle	Angle between Rotation Axes		
		Gi	Gx	Gy
Gi	0.000014 ± 0.000013		-	-
Gx	0.499968 ± 0.000019	-		0.499997π
Gy	0.499996 ± 0.000018	-	0.499997π	

Table 9: **Eigen-decomposition of estimated gates.** Each estimated gate is described in terms of: (1) the eigenvalues of the superoperator; (2) the gate’s fixed point (as a vector in $\mathcal{B}(\mathcal{H})$, in the Pauli basis); (3) the axis around which it rotates, as a vector in $\mathcal{B}(\mathcal{H})$; (4) the angle of the rotation that it applies; (5) the decay rate along the axis of rotation (“diagonal decay”); (6) the decay rate perpendicular to the axis of rotation (“off-diagonal decay”); and (7) the angle between each gate’s rotation axis and the rotation axes of the other gates. “X” indicates that the decomposition failed or couldn’t be interpreted.

Gate	Process Infidelity	$1/2$ -width Trace Distance	Rotation Axis	Rotation Angle	Sanity ✓
Gi	0.000041	0.000045	0 0.0262 0.0817 -0.9963	0.000016π	0.000001
Gx	0.000054	0.000054	0 1 -5×10^{-6} 6×10^{-7}	0.499968π	0.000001
Gy	0.000069	0.000069	0 -5×10^{-6} 1 1×10^{-7}	0.499996π	1×10^{-7}

Table 10: Information pertaining to the closest unitary gate to each of the estimated gates.

Gate	Choi matrix (Pauli basis)	Eigenvalues	
Gi	$\begin{pmatrix} 1 & 1 \times 10^{-6}e^{i2.5} & 5 \times 10^{-6}e^{-i0.5} & 3 \times 10^{-5}e^{-i1.4} \\ 1 \times 10^{-6}e^{-i2.5} & 2 \times 10^{-5} & 5 \times 10^{-6}e^{-i1.9} & 2 \times 10^{-5}e^{i2.9} \\ 5 \times 10^{-6}e^{i0.5} & 5 \times 10^{-6}e^{i1.9} & 1 \times 10^{-6} & 1 \times 10^{-6}e^{i2.2} \\ 3 \times 10^{-5}e^{i1.4} & 2 \times 10^{-5}e^{-i2.9} & 1 \times 10^{-6}e^{-i2.2} & 2 \times 10^{-5} \end{pmatrix}$	-3×10^{-6} 6×10^{-6} 4×10^{-5} 1	1×10^{-5} $\pm 1 \times 10^{-5}$ 2×10^{-5} 1×10^{-5}
Gx	$\begin{pmatrix} 0.5 & 0.5e^{-i1.6} & 9 \times 10^{-6}e^{-i1.8} & 4 \times 10^{-6}e^{-i1.1} \\ 0.5e^{i1.6} & 0.4999 & 5 \times 10^{-6}e^{-i2.7} & 4 \times 10^{-6}e^{-i2.6} \\ 9 \times 10^{-6}e^{i1.8} & 5 \times 10^{-6}e^{i2.7} & 2 \times 10^{-5} & 4 \times 10^{-6}e^{i1.5} \\ 4 \times 10^{-6}e^{i1.1} & 4 \times 10^{-6}e^{i2.6} & 4 \times 10^{-6}e^{-i1.5} & 8 \times 10^{-6} \end{pmatrix}$	5×10^{-6} 1×10^{-5} 3×10^{-5} 0.9999	2×10^{-5} $\pm 3 \times 10^{-5}$ 3×10^{-5} 1×10^{-5}
Gy	$\begin{pmatrix} 0.5 & 9 \times 10^{-6}e^{i1.4} & 0.4999e^{i1.6} & 4 \times 10^{-6}e^{-i2.1} \\ 9 \times 10^{-6}e^{-i1.4} & 2 \times 10^{-5} & 4 \times 10^{-6}e^{i2.7} & 3 \times 10^{-7}e^{-i2.3} \\ 0.4999e^{-i1.6} & 4 \times 10^{-6}e^{-i2.7} & 0.5 & 4 \times 10^{-6}e^{-i0.5} \\ 4 \times 10^{-6}e^{i2.1} & 3 \times 10^{-7}e^{i2.3} & 4 \times 10^{-6}e^{i0.5} & 3 \times 10^{-6} \end{pmatrix}$	3×10^{-6} 1×10^{-5} 0.0001 0.9999	2×10^{-5} $\pm 3 \times 10^{-5}$ 2×10^{-5} 1×10^{-5}

Table 11: **Choi matrix representation of the GST estimated gateset.** This table lists Choi representations of the estimated gates, and their eigenvalues. Unitary gates have a spectrum $(1, 0, 0 \dots)$, just like pure quantum states. Negative eigenvalues are non-physical, and may represent either statistical fluctuations or violations of the CPTP model used by GST.

4 Goodness-of-model Analysis

The previous section presented the estimated gateset, and compared it to the target gateset. This section is concerned with a mostly orthogonal analysis which seeks to explain how much the estimated gateset can be trusted – i.e., how well it fits the data.

To understand the goal of this section, consider the simple problem of fitting a line to a set of points. For any set of points, there is *always* a best-fit line – but this doesn’t mean that the best-fit line is a *good* fit! The data points may trace out a parabola, a square, or even something more complicated. It is essential to understand not just what the best-fit line was (and perhaps how close it was to some desired line), but also **how well that linear model was able to fit all the data**. Of course, we do not expect it to fit every data point perfectly. The critical question is “Did the linear model fit *as well as we would expect it to* if the data really were generated by a linear process?”

In this analogy, GST’s estimated gateset is like the best-fit line, and the target gateset like the desired line. This section asks the question “How well was GST able to fit all of the data – and did it fit well enough to suggest that its model is valid?” A central tool used to do this is the *likelihood function*, which we denote \mathcal{L} , which formally is the probability of the observed data given a set of model parameters. The basic idea is that we maximize the likelihood function to obtain the best set of model parameters (i.e. gate set), and by looking at the value of this maximum we can determine the model’s goodness-of-fit. We will actually deal primarily with the logarithm of the likelihood function, $\log(\mathcal{L})$, which is similarly maximized.

4.1 Aggregated $\log(\mathcal{L})$

The log-likelihood for an n -outcome system with predicted probabilities p_i and observed frequencies f_i ($i = 1 \dots n$) is given by:

$$\log(\mathcal{L}) = \sum_i N f_i \log(p_i). \quad (1)$$

where N is the total number of counts. In *this* analysis, $\log(\mathcal{L})$ is used to compare the set of probabilities predicted by a gateset (p_s) and the frequencies obtained from a dataset (f_s). Each experiment (or gate sequence) s is associated to two probabilities: “plus” has probability p_s and “minus” has probability $1 - p_s$. The $\log(\mathcal{L})$ contribution of a single gate string s is

$$\log(\mathcal{L})_s = N f_s \log(p_s) + N(1 - f_s) \log(1 - p_s), \quad (2)$$

where N is the number of times the experiment s was performed, p_s is the probability of a “plus” outcome as predicted by the gateset, and f_s is the observed frequency of “plus”. The total log-likelihood for an entire dataset is just the sum

$$\log(\mathcal{L}) = \sum_{s \in \mathcal{S}} \log(\mathcal{L})_s. \quad (3)$$

A theoretical upper bound on the log-likelihood can be found by replacing p_s with f_s in Eq. 2 and evaluating Eq. 3. We will refer to this quantity as $\log(\mathcal{L})_{ub}$.

Statistical theory has quite a lot to say about the likelihood function (see any of the major textbooks). Using some of these results, we can predict that if there are N_p free parameters in the gateset that GST is fitting, and GST fits a dataset containing $N_s > N_p$ distinct experiments (gate sequences), then *if the gateset model is correct*, then two times the difference between $\log(\mathcal{L})_{ub}$ and the maximum $\log(\mathcal{L})$ obtained is a random variable with a χ^2_k distribution, where

$$k \equiv N_s - N_p.$$

Its expected value is $\langle \chi^2 \rangle = k$, and its RMS variance is $\pm\sqrt{2k}$. Thus, if the fit is “good”, then twice $\Delta \log(\mathcal{L}) \equiv \log(\mathcal{L})_{ub} - \max(\log(\mathcal{L}))$ should lie roughly within the interval $[k - \sqrt{2k}, k + \sqrt{2k}]$ where $k = N_s - N_p$. Thus, by comparing the difference $2\Delta \log(\mathcal{L}) - k$ to $\sqrt{2k}$ one can determine how well the GST estimate was able to fit the data in dataset “GSTBest_condensed”.

The MLEGST algorithm used to generate this estimate is iterative. It starts by fitting only data from the shortest gate sequences (which are easy to fit *and* insensitive to most non-Markovian noise), then successively

adds longer and longer sequences (with base sequence length $L \leq 1, 2, 4, 8, \dots$) to the mix. Since we get an estimate at each intermediate L , it is possible to quantify not just the goodness of the *best* fit (presented in the previous section), but how the goodness-of-fit behaves as longer and longer sequences are added in.

This data is presented in Table 12. What you should be looking for here is whether – at each value of L – the $2\Delta \log(\mathcal{L})$ quantity is roughly the same as k . More precisely, is $|2\Delta \log(\mathcal{L}) - k|$ less than or equal to $\sqrt{2k}$? If not, then the model is not fitting as well as it should, which usually indicates non-Markovian noise (or, rarely, that the GST algorithm has simply failed to find a good fit even though one exists).

As a rough rule of thumb, for GST experiments involving relatively long sequences (e.g. $L \geq 100$):

- “Incredibly good” (★★★★★) experiments have $2\Delta \log(\mathcal{L}) \approx k$, as predicted by theory (and seen in simulations).
- “Great” (★★★★) experiments have $2\Delta \log(\mathcal{L}) \leq 2k$ or so.
- “Good” (★★★) experiments have $2\Delta \log(\mathcal{L}) \leq 5k$ or so.
- “Okay” (★★) experiments have $2\Delta \log(\mathcal{L}) \leq 10k$.
- Experiments in which $2\Delta \log(\mathcal{L}) > 10k$ (★) have very significant non-Markovian noise, and the results in the previous section should be viewed very cautiously.

L	$2\Delta \log(\mathcal{L})$	k	$2\Delta \log(\mathcal{L}) - k$	$\sqrt{2k}$	P	N_s	N_p	Rating
1	59.47348	61	-1.526521	11.04536	0.53	92	31	★★★★★
2	144.2938	137	7.293755	16.55295	0.32	168	31	★★★★★
4	422.7099	410	12.70986	28.63564	0.32	441	31	★★★★★
8	779.8896	786	-6.110415	39.64846	0.55	817	31	★★★★★
16	1192.721	1170	22.72143	48.37355	0.32	1201	31	★★★★★
32	1598.682	1554	44.68206	55.74944	0.21	1585	31	★★★★★
64	1960.273	1938	22.27336	62.25753	0.36	1969	31	★★★★★
128	2335.643	2322	13.64338	68.1469	0.42	2353	31	★★★★★
256	2759.649	2706	53.6495	73.5663	0.23	2737	31	★★★★★
512	3172.446	3090	82.44637	78.61298	0.15	3121	31	★★★★
1024	3707.829	3474	233.829	83.35466	3×10^{-3}	3505	31	★★★★
2048	4128.229	3858	270.229	87.84077	1×10^{-3}	3889	31	★★★★
4096	4327.875	4242	85.87503	92.10863	0.18	4273	31	★★★★★

Table 12: **Comparison between the computed and expected maximum $\log(\mathcal{L})$ for different values of L .** N_s and N_p are the number of gate strings and parameters, respectively. The quantity $2\Delta \log(\mathcal{L})$ measures the goodness of fit of the GST model (small is better) and is expected to lie within $[k - \sqrt{2k}, k + \sqrt{2k}]$ where $k = N_s - N_p$. P is the p-value derived from a χ_k^2 distribution (i.e. when $P <$ some threshold like 0.05 there is grounds for rejecting the GST fit). The rating from 1 to 5 stars gives a very crude indication of goodness of fit as explained in the text.

4.2 Detailed likelihood analysis

The aggregated $2\Delta \log(\mathcal{L})$ numbers presented in Table 12 tell you how well the GST estimate fits the *entire* dataset. If they are in line with theory ($2\Delta \log(\mathcal{L}) \approx k$), then there is little more to be said. But if the best fit to the data is not good, we can debug it by identifying *which* experiments are inconsistent with the fit.

Figure 1 displays the $2\Delta \log(\mathcal{L})$ contribution from each individual gate sequence (Eq. 2). Each gate sequence corresponds to a single colored “pixel” in the plot. Each block of pixels corresponds to a single base sequence (i.e., a germ power), and the individual pixels within a block correspond to the various fiducial sequence pairs between which that base sequence was sandwiched. (The column indicates the fiducial adjacent to state preparation, while the row indicates the fiducial adjacent to measurement). Base sequences

are arranged in a grid; different rows correspond to different germs, while different columns correspond to different maximum lengths L . Pixels are labeled with the $2\Delta \log(\mathcal{L})$ contribution for that sequence, and colored appropriately. Shades of blue indicate $2\Delta \log(\mathcal{L})$ contributions in the range 0-3 (“consistent”), while dark red indicates a $2\Delta \log(\mathcal{L})$ contribution of 10 or above. Such events ($2\Delta \log(\mathcal{L})_s \geq 10$) should occur only once per 638 experiments if the model is correct.

Identifying patterns and trends within such “pixel plots” can aid in identifying specific sources and types of non-Markovian noise which may be to blame if the GST algorithms are unable to produce a “good” estimate. For example, it is often the case that all the short sequences [$L = O(1)$] can be fit reasonably well, but the right-hand side of Figure 1 becomes a sea of red. This indicates that non-Markovian behavior (potentially due to slow drift of gateset parameters) is becoming more significant for longer experiments. In other cases, a single row may be particularly bad, indicating that a particular gate or germ is especially problematic (e.g., was not stabilized using dynamical decoupling techniques). Be cautious in debugging, however – sometimes bad $\log(\mathcal{L})$ values for a particular gate or germ can result *not* from faults in that operation, but because another operation failed so badly that it distorted the entire fit (e.g., in trying to fit catastrophically non-Markovian data at Point A, GST ended up failing to fit perfectly good data at Point B).

If the “generate appendices” option was selected for this report, similar pixel plots for the intermediate estimates whose total $2\Delta \log(\mathcal{L})$ is listed in Table 12 can be found in Appendix B.

Figure 2 shows exactly the same $\log(\mathcal{L})$ analysis as Figure 1, but arranged differently. Here, blocks (not square) all correspond to a single fiducial pair (e.g., pre- and post-fiducial), and pixels within a block correspond to different base sequences. This can be useful for diagnosing a single bad fiducial sequence.

4.3 Debugging aids

If the $\log(\mathcal{L})$ plots in Figures 1-2 indicate that the data is poorly fit by GST, the next step is to begin “debugging” the experiments and/or the fit. Most commonly, a poor fit is due to non-Markovian behavior. However, there are many kinds of non-Markovian behavior. The most straightforward occurs when the gateset fluctuates over time, or when there is other time correlation in the experiments (e.g., due to memory effects). However, another possibility that must be considered is that repeated gate operations cause changes in the system, e.g. heating it up (as is seen in 2-qubit trapped-ion gates) so that the data from long gate sequences is simply chaotic and inconsistent with shorter experiments.

Figure 3 provides a test (albeit currently an unreliable one) for such an effect. Like Figures 1-2, it displays per-experiment $2\Delta \log(\mathcal{L})$ values – but *not* for any single gateset. Instead, this *direct GST* analysis treats each base sequence as an independent process (*not* as a product of many gates), and analyzes it using LSGST together with the individual gates (which are necessary to model the effect of the fiducial sequences that precede and follow the base sequence being analyzed). The resulting direct GST estimate is then used to assign probabilities for the corresponding experiments.

This analysis decouples the various germs and base sequences from each other. Unlike a standard GST analysis, it does not model different base sequences as being generated from the same gates. Therefore, this analysis *should* be fairly consistent (i.e., lots of blue squares and few or no red ones) even if Figures 1-2 indicate severe fit problems.

Figure 4 uses direct GST analysis in another way, but to detect similar effects. The goal here is to compare two different predictions for each base sequence: (1) the one given by the overall GST fit; and (2) the one obtained by direct GST on that base sequence, as in Figure 3. The analysis shown in Figure 4 does so by computing each process’s fidelity with the closest unitary. This is a measure of non-unitary decoherence. Then, it plots the *difference* between the values of this “unitarity” for (1) the overall GST fit, and (2) the direct GST estimate. The direct GST estimate is not very precise, but it is extremely reliable, because it is not influenced by any data that are not *directly* connected with that base sequence. Thus, this serves as another sanity check and debugging aid. Large absolute values indicate that the full GST fit is significantly inconsistent with the data (complementing the analysis in Figure 1). Positive numbers indicate that full GST has *overestimated* the amount of decoherence, while negative numbers indicate that it *underestimated* it.

Finally, for various reasons including the diagnosis of non-Markovian behavior, it is often useful to have a direct and reliable estimate of the per-gate incoherent error rate observed in each base sequence. This is

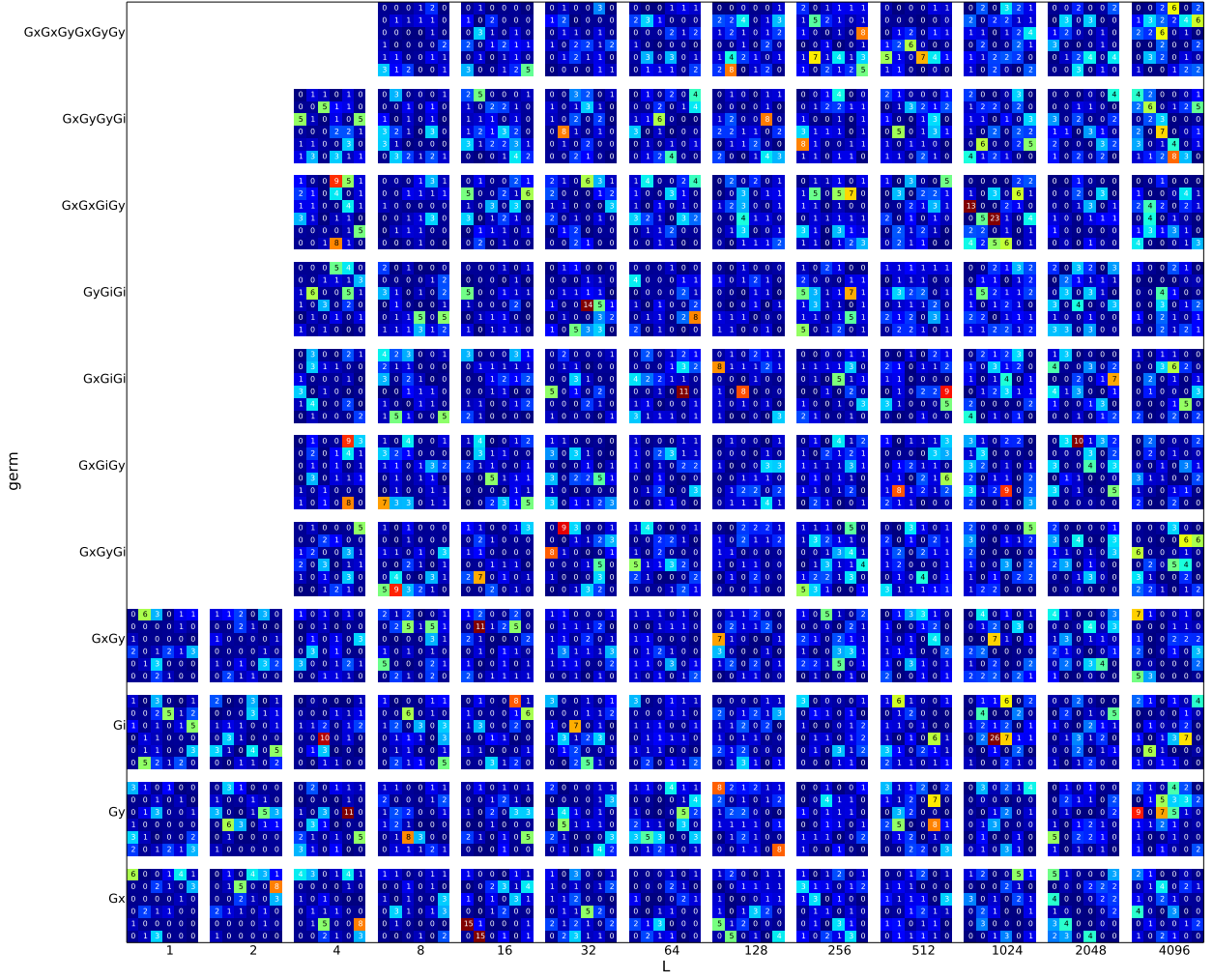


Figure 1: $2\Delta \log(\mathcal{L})$ contributions for every individual experiment in the dataset. Each pixel represents a single experiment (gate sequence), and its color indicates whether GST was able to fit the corresponding frequency well. Blue is typical; dark red squares indicating $2\Delta \log(\mathcal{L})_s > 10$ should appear only once per 638 experiments on average. Square blocks of pixels correspond to base sequences (arranged vertically by germ and horizontally by length); each pixel within a block corresponds to a specific choice of pre- and post-fiducial sequences. See text for further details.

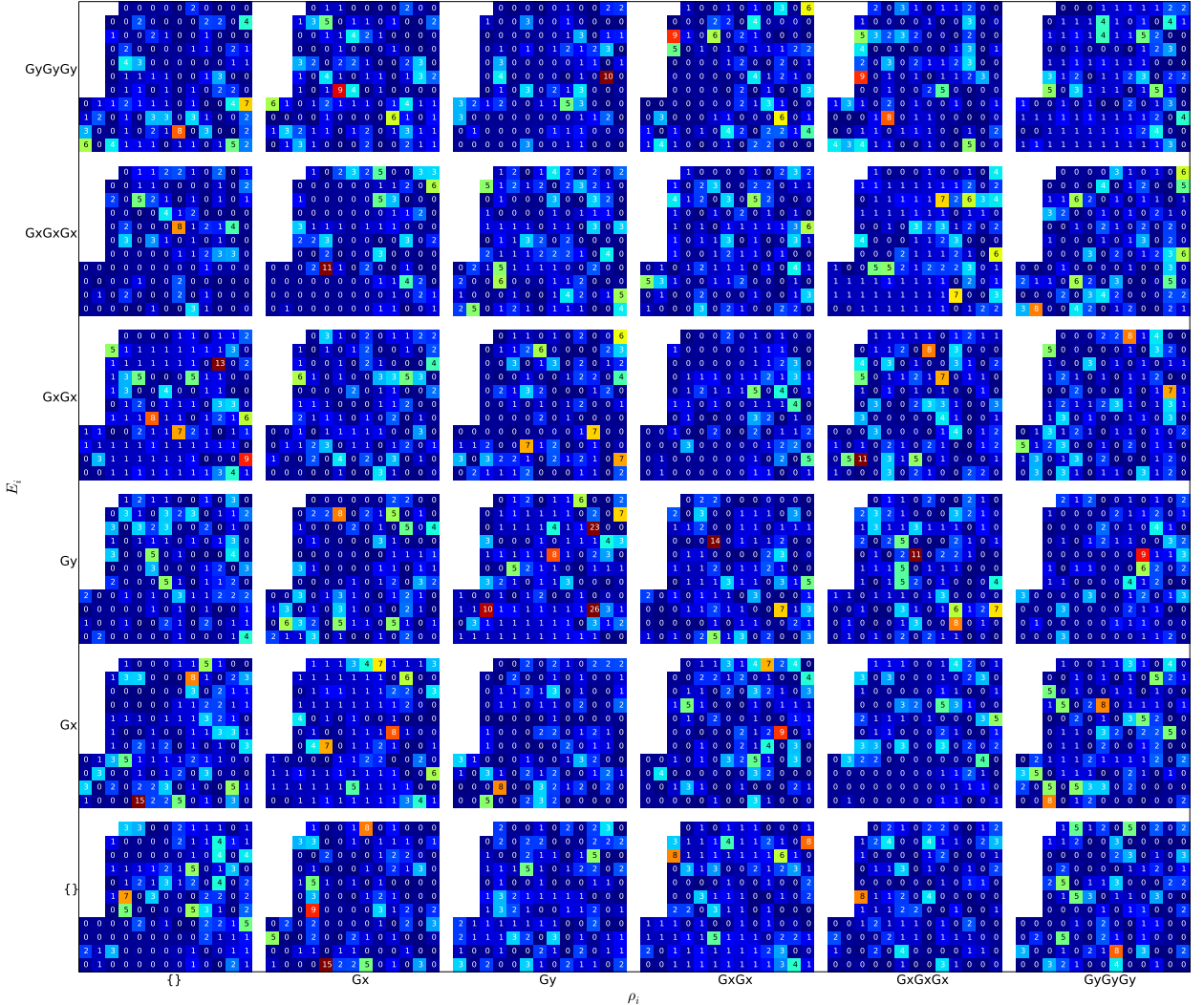


Figure 2: $2\Delta \log(\mathcal{L})$ contributions for each experiment, arranged differently. This figure shows the same data as Figure 1, but arranged differently. Each block now corresponds to a particular pair of fiducial sequences, while pixels within the block correspond to different base sequences sandwiched between those fiducials.

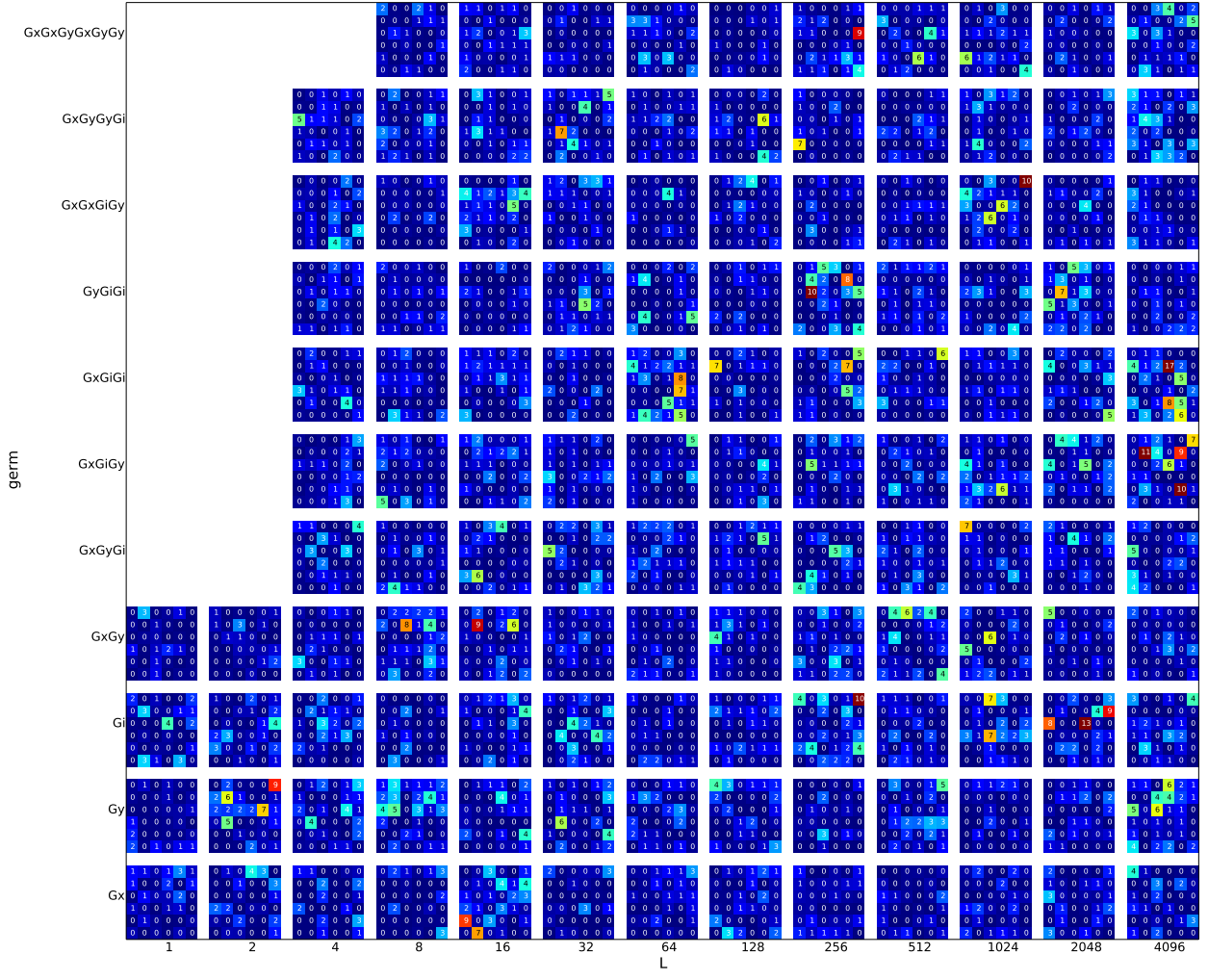


Figure 3: $2\Delta \log(\mathcal{L})$ values for “direct GST” fit. This plot indicates how well direct GST analysis of each base sequence fits the observed data. By decoupling different base sequences, this analysis largely avoids making any assumptions about Markovianity, and therefore serves as a sanity check on the full GST analysis. See text for details.

shown in Figure 5. To obtain these numbers, direct GST is performed on each base sequence. Then, each resulting process matrices is diagonalized, and the smallest eigenvalue (corresponding the most rapid loss of information/coherence/polarization) is extracted. This eigenvalue is then raised to the $1/L$ power, where L is the length of the base sequence, to estimate the rate of decoherence per gate, and subtracted from 1 (to convert it to an error rate). These numbers become much more reliable towards the right-hand side of the plot, because errors in LGST become far less significant for these long sequences. Large changes in this direct-GST error rate as L is changed (on any given row of the table) are a “smoking gun” for non-Markovian decoherence – especially when the error rate *decreases* with increasing L . Ideally, all numbers in a given row should be the same.

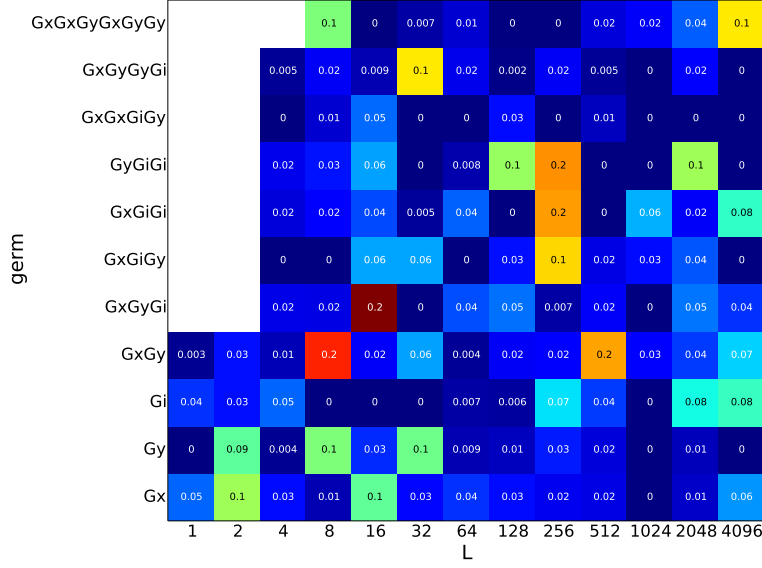


Figure 4: **Inconsistency of unitarity between GST and direct GST.** This plot shows, for each base sequence, the increase in “upper bound of fidelity with unitary” (see Table 10) when using the direct-GST result for a gate sequence instead of the process given by the best gateset.

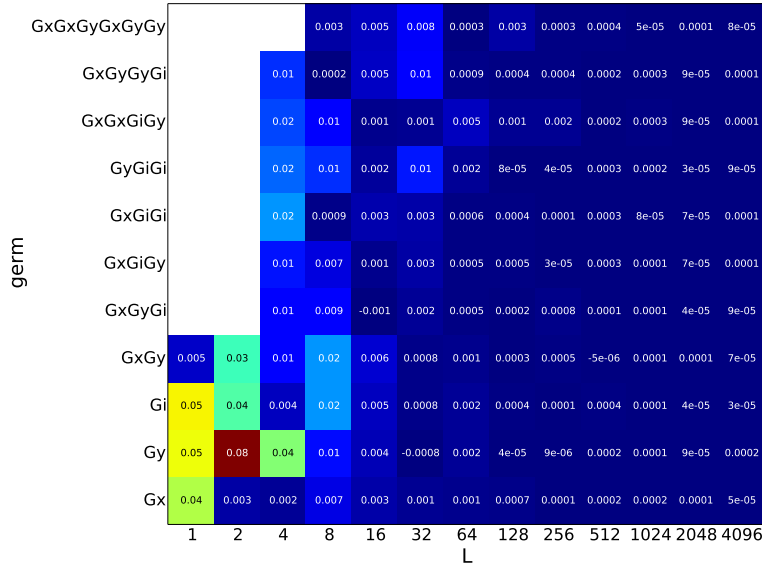


Figure 5: **Per-gate error rates, extrapolated from the smallest magnitude eigenvalue of the direct GST gate matrix.** See text for further details.

A Best gateset in different gauges

In this appendix, we report the non-gauge-invariant quantities from the main text for different gauge choices. In each section, GST's best gateset estimate is gauge optimized according to a different objective function, as specified within the section.

A.1 Gauge optimization to the target gateset

The gauge is chosen to minimize the Frobenius distance between the estimate and the target gates, with equal weight given to the gate and SPAM parameters.

Operator	Hilbert-Schmidt vector (Pauli basis)	Matrix
ρ_0	0.7071 0.0046 −0.0032 0.7016	$\begin{pmatrix} 0.9961 & 0.004e^{i0.6} \\ 0.004e^{-i0.6} & 0.0039 \end{pmatrix}$
E_0	0.7023 −0.0003 −0.0005 −0.7017	$\begin{pmatrix} 0.0004 & 0.0004e^{i2.2} \\ 0.0004e^{-i2.2} & 0.9928 \end{pmatrix}$

Table 13: **The GST estimate of the SPAM operations.** Compare to Table 1.

	E_0	E_{-1}
ρ_0	0.004272	0.995728

Table 14: **GST estimate of SPAM probabilities.** Computed by taking the dot products of vectors in Table 13.

Gate	Superoperator (Pauli basis)
G_i	$\begin{pmatrix} 1 & 0 & 0 & 0 \\ -4 \times 10^{-6} & 1 & -5 \times 10^{-5} & -4 \times 10^{-5} \\ -2 \times 10^{-5} & 0.0001 & 0.9999 & 3 \times 10^{-6} \\ 2 \times 10^{-5} & -3 \times 10^{-5} & -1 \times 10^{-7} & 1 \end{pmatrix}$
G_x	$\begin{pmatrix} 1 & 0 & 0 & 0 \\ -2 \times 10^{-5} & 0.9999 & -0.0011 & 0.0011 \\ 0.003 & 0.0006 & 0.0005 & -0.9999 \\ 0.0007 & 0.0006 & 0.9999 & -0.0003 \end{pmatrix}$
G_y	$\begin{pmatrix} 1 & 0 & 0 & 0 \\ -0.0034 & 0.0005 & 0.0003 & 0.9999 \\ 1 \times 10^{-6} & -0.0007 & 1 & -0.0007 \\ 0.0002 & -0.9999 & -0.0003 & -0.0005 \end{pmatrix}$

Table 15: **The GST estimate of the logic gate operations.** Compare to Table 2.

Gate	Process Infidelity	$1/2$ -width Trace Distance	$1/2$ -width \diamond -Norm	Frobenius Distance
Gi	0.000041	0.000052	0.00006	0.000136
Gx	0.000054	0.001734	0.002039	0.003598
Gy	0.000069	0.001807	0.002035	0.003664

Gate	Error Generator
Gi	$\begin{pmatrix} 0 & 0 & 0 & 0 \\ -4 \times 10^{-6} & -5 \times 10^{-5} & -5 \times 10^{-5} & -4 \times 10^{-5} \\ -2 \times 10^{-5} & 0.0001 & -0.0001 & 3 \times 10^{-6} \\ 2 \times 10^{-5} & -3 \times 10^{-5} & -1 \times 10^{-7} & -4 \times 10^{-5} \end{pmatrix}$
Gx	$\begin{pmatrix} 0 & 0 & 0 & 0 \\ -2 \times 10^{-5} & -0.0001 & -0.0011 & 0.0011 \\ 0.0007 & 0.0006 & -0.0001 & -0.0003 \\ -0.003 & -0.0006 & -0.0005 & -0.0001 \end{pmatrix}$
Gy	$\begin{pmatrix} 0 & 0 & 0 & 0 \\ -0.0002 & -0.0001 & 0.0003 & 0.0005 \\ -2 \times 10^{-7} & -0.0007 & -4 \times 10^{-5} & -0.0007 \\ -0.0034 & 0.0005 & 0.0003 & -0.0001 \end{pmatrix}$

Table 16: **Comparison of GST estimated gates to target gates.** This table presents, for each of the gates, three different measures of distance or discrepancy from the GST estimate to the ideal target operation. See text for more detail. The column labeled “Error Generator” gives the Lindbladian \mathcal{L} that describes *how* the gate is failing to match the target. This error generator is defined by the equation $\hat{G} = G_{\text{target}}e^{\mathcal{L}}$.

Gate	Eigenvalues	Fixed pt	Rotn. axis	Diag. decay	Off-diag. decay
Gi	1	1	0	0.000018	0.000073
	$0.9999e^{i0.0}$	0	0.4712		
	$0.9999e^{-i0.0}$	0	0.3834		
	1	0	-0.7943		
Gx	$0.9999e^{i1.6}$	1	0	0.000056	0.00008
	$0.9999e^{-i1.6}$	-1×10^{-6}	1		
	0.9999	0.0011	7×10^{-6}		
	1	0.0018	0.0006		
Gy	$0.9999e^{i1.6}$	1	0	0.000039	0.000118
	$0.9999e^{-i1.6}$	-0.0016	-7×10^{-6}		
	1	5×10^{-7}	1		
	1	0.0018	-0.0003		

Gate	Angle	Angle between Rotation Axes		
		Gi	Gx	Gy
Gi	0.000014		—	—
Gx	0.499968	—		0.5π
Gy	0.499996	—	0.5π	

Table 17: **Eigen-decomposition of estimated gates.** Each estimated gate is described in terms of: (1) the eigenvalues of the superoperator; (2) the gate’s fixed point (as a vector in $\mathcal{B}(\mathcal{H})$, in the Pauli basis); (3) the axis around which it rotates, as a vector in $\mathcal{B}(\mathcal{H})$; (4) the angle of the rotation that it applies; (5) the decay rate along the axis of rotation (“diagonal decay”); and (6) the decay rate perpendicular to the axis of rotation (“off-diagonal decay”). “—” indicates that the decomposition failed or couldn’t be interpreted.

Gate	Process Infidelity	$^{1/2}$ -width Trace Distance	Rotation Axis	Rotation Angle	Sanity ✓
Gi	0.000041	0.000045	0 0.0274 0.0809 -0.9963	0.000016 π	0.000001
Gx	0.000054	0.001549	0 -1 4×10^{-6} -0.0009	0.499968 π	0.010788
Gy	0.000069	0.001746	0 4×10^{-6} -1 0.0005	0.499996 π	0.010862

Table 18: Information pertaining to the closest unitary gate to each of the estimated gates.

Gate	Choi matrix (Pauli basis)	Eigenvalues
Gi	$\begin{pmatrix} 1 & 1 \times 10^{-6}e^{i2.5} & 5 \times 10^{-6}e^{-i0.5} & 3 \times 10^{-5}e^{-i1.4} \\ 1 \times 10^{-6}e^{-i2.5} & 2 \times 10^{-5} & 5 \times 10^{-6}e^{-i1.9} & 2 \times 10^{-5}e^{i2.9} \\ 5 \times 10^{-6}e^{i0.5} & 5 \times 10^{-6}e^{i1.9} & 1 \times 10^{-6} & 1 \times 10^{-6}e^{i2.2} \\ 3 \times 10^{-5}e^{i1.4} & 2 \times 10^{-5}e^{-i2.9} & 1 \times 10^{-6}e^{-i2.2} & 2 \times 10^{-5} \end{pmatrix}$	-3×10^{-6} 6×10^{-6} 4×10^{-5} 1
Gx	$\begin{pmatrix} 0.5 & 0.5e^{-i1.6} & 0.0007e^{i3.0} & 0.0005e^{-i1.2} \\ 0.5e^{i1.6} & 0.4999 & 0.0002e^{-i1.0} & 0.0009e^{-i1.0} \\ 0.0007e^{-i3.0} & 0.0002e^{i1.0} & 0.0002 & 7 \times 10^{-6}e^{i2.4} \\ 0.0005e^{i1.2} & 0.0009e^{i1.0} & 7 \times 10^{-6}e^{-i2.4} & -0.0002 \end{pmatrix}$	-0.0008 0.0001 0.0008 0.9999
Gy	$\begin{pmatrix} 0.5 & 0.0009e^{-i3.0} & 0.4999e^{i1.6} & 0.0002e^{i1.4} \\ 0.0009e^{i3.0} & 0.0003 & 0.0001e^{-i0.4} & 8 \times 10^{-6}e^{-i3.1} \\ 0.4999e^{-i1.6} & 0.0001e^{i0.4} & 0.5 & 0.0009e^{i1.3} \\ 0.0002e^{-i1.4} & 8 \times 10^{-6}e^{i3.1} & 0.0009e^{-i1.3} & -0.0002 \end{pmatrix}$	-0.0009 2×10^{-5} 0.0009 0.9999

Table 19: **Choi matrix representation of the GST estimated gateset.** This table lists Choi representations of the estimated gates, and their eigenvalues. Unitary gates have a spectrum $(1, 0, 0 \dots)$, just like pure quantum states. Negative eigenvalues are non-physical, and may represent either statistical fluctuations or violations of the CPTP model used by GST.

A.2 Gauge optimization to the target SPAM

The gauge is chosen to minimize the Frobenius distance between the estimate and the target gates, with 99% weight given to the SPAM parameters, 1% to the gate parameters.

Operator	Hilbert-Schmidt vector (Pauli basis)	Matrix
ρ_0	0.7071 0.0002 -0.0001 0.7049	$\begin{pmatrix} 0.9984 & 0.0001e^{i0.6} \\ 0.0001e^{-i0.6} & 0.0016 \end{pmatrix}$
E_0	0.7087 3×10^{-5} -0.0001 -0.7049	$\begin{pmatrix} 0.0027 & 0.0001e^{i1.2} \\ 0.0001e^{-i1.2} & 0.9996 \end{pmatrix}$

Table 20: **The GST estimate of the SPAM operations.** Compare to Table 1.

	E_0	E_{-1}
ρ_0	0.004272	0.995728

Table 21: **GST estimate of SPAM probabilities.** Computed by taking the dot products of vectors in Table 20.

Gate	Superoperator (Pauli basis)
G_i	$\begin{pmatrix} 1 & 0 & 0 & 0 \\ -3 \times 10^{-6} & 1 & -5 \times 10^{-5} & -4 \times 10^{-5} \\ -2 \times 10^{-5} & 0.0001 & 0.9999 & 3 \times 10^{-6} \\ 2 \times 10^{-5} & -3 \times 10^{-5} & -2 \times 10^{-7} & 1 \end{pmatrix}$
G_x	$\begin{pmatrix} 1 & 0 & 0 & 0 \\ -4 \times 10^{-5} & 0.9999 & -0.0034 & 0.0033 \\ 0.0152 & 0.0012 & 0.0024 & -0.9998 \\ 0.0066 & 0.0012 & 1 & -0.0022 \end{pmatrix}$
G_y	$\begin{pmatrix} 1 & 0 & 0 & 0 \\ -0.0165 & 0.0022 & -0.0003 & 0.9997 \\ 1 \times 10^{-5} & -0.0019 & 1 & -0.0019 \\ 0.0053 & -1 & 0.0003 & -0.0022 \end{pmatrix}$

Table 22: **The GST estimate of the logic gate operations.** Compare to Table 2.

Gate	Process Infidelity	$1/2$ -width Trace Distance	$1/2$ -width \diamond -Norm	Frobenius Distance
Gi	0.000041	0.000052	0.00006	0.000136
Gx	0.000055	0.008705	0.009876	0.017633
Gy	0.000067	0.008855	0.009848	0.017847

Gate	Error Generator			
Gi	$\begin{pmatrix} 0 & 0 & 0 & 0 \\ -3 \times 10^{-6} & -5 \times 10^{-5} & -5 \times 10^{-5} & -4 \times 10^{-5} \\ -2 \times 10^{-5} & 0.0001 & -0.0001 & 3 \times 10^{-6} \\ 2 \times 10^{-5} & -3 \times 10^{-5} & -2 \times 10^{-7} & -4 \times 10^{-5} \end{pmatrix}$			
Gx	$\begin{pmatrix} 0 & 0 & 0 & 0 \\ -3 \times 10^{-6} & -0.0001 & -0.0034 & 0.0033 \\ 0.0066 & 0.0012 & 3 \times 10^{-5} & -0.0022 \\ -0.0152 & -0.0012 & -0.0024 & -0.0002 \end{pmatrix}$			
	$\begin{pmatrix} 0 & 0 & 0 & 0 \\ -0.0052 & 3 \times 10^{-5} & -0.0003 & 0.0022 \\ -1 \times 10^{-5} & -0.0019 & -4 \times 10^{-5} & -0.0019 \\ -0.0165 & 0.0022 & -0.0003 & -0.0003 \end{pmatrix}$			

Table 23: **Comparison of GST estimated gates to target gates.** This table presents, for each of the gates, three different measures of distance or discrepancy from the GST estimate to the ideal target operation. See text for more detail. The column labeled “Error Generator” gives the Lindbladian \mathcal{L} that describes *how* the gate is failing to match the target. This error generator is defined by the equation $\hat{G} = G_{\text{target}}e^{\mathcal{L}}$.

Gate	Eigenvalues	Fixed pt	Rotn. axis	Diag. decay	Off-diag. decay
Gi	1	1	0		
	$0.9999e^{i0.0}$	0	0.4729	0.000018	0.000073
	$0.9999e^{-i0.0}$	0	0.3824		
	1	0	-0.7938		
Gx	$0.9999e^{i1.6}$	0.9999	0		
	$0.9999e^{-i1.6}$	-1×10^{-5}	1	0.000056	0.00008
	0.9999	0.0043	1×10^{-5}		
	1	0.0109	0.0012		
Gy	$0.9999e^{i1.6}$	0.9998	0		
	$0.9999e^{-i1.6}$	-0.0057	-4×10^{-6}	0.000039	0.000118
	1	-4×10^{-6}	1		
	1	0.0109	0.0003		

Gate	Angle	Angle between Rotation Axes		
		Gi	Gx	Gy
Gi	0.000014		—	—
Gx	0.499968	—		0.499998π
Gy	0.499996	—	0.499998π	

Table 24: **Eigen-decomposition of estimated gates.** Each estimated gate is described in terms of: (1) the eigenvalues of the superoperator; (2) the gate’s fixed point (as a vector in $\mathcal{B}(\mathcal{H})$, in the Pauli basis); (3) the axis around which it rotates, as a vector in $\mathcal{B}(\mathcal{H})$; (4) the angle of the rotation that it applies; (5) the decay rate along the axis of rotation (“diagonal decay”); and (6) the decay rate perpendicular to the axis of rotation (“off-diagonal decay”). “—” indicates that the decomposition failed or couldn’t be interpreted.

Gate	Process Infidelity	$^{1/2}$ -width Trace Distance	Rotation Axis	Rotation Angle	Sanity ✓
Gi	0.000041	0.000045	0 0.0297 0.0811 -0.9963	0.000016 π	0.000001
Gx	0.000052	0.008416	0 -1 3×10^{-6} -0.0023	0.499968 π	0.492374
Gy	0.000067	0.008795	0 3×10^{-6} -1 0.0008	0.499996 π	0.392521

Table 25: Information pertaining to the closest unitary gate to each of the estimated gates.

Gate	Choi matrix (Pauli basis)	Eigenvalues
Gi	$\begin{pmatrix} 1 & 1 \times 10^{-6}e^{i2.4} & 4 \times 10^{-6}e^{-i0.5} & 3 \times 10^{-5}e^{-i1.4} \\ 1 \times 10^{-6}e^{-i2.4} & 2 \times 10^{-5} & 5 \times 10^{-6}e^{-i1.9} & 2 \times 10^{-5}e^{i2.9} \\ 4 \times 10^{-6}e^{i0.5} & 5 \times 10^{-6}e^{i1.9} & 1 \times 10^{-6} & 1 \times 10^{-6}e^{i2.2} \\ 3 \times 10^{-5}e^{i1.4} & 2 \times 10^{-5}e^{-i2.9} & 1 \times 10^{-6}e^{-i2.2} & 2 \times 10^{-5} \end{pmatrix}$	-3×10^{-6} 6×10^{-6} 4×10^{-5} 1
Gx	$\begin{pmatrix} 0.5 & 0.5e^{-i1.6} & 0.0038e^{i3.0} & 0.002e^{-i0.6} \\ 0.5e^{i1.6} & 0.4999 & 0.0017e^{-i1.3} & 0.004e^{-i1.3} \\ 0.0038e^{-i3.0} & 0.0017e^{i1.3} & 0.0012 & 0.0001e^{i3.0} \\ 0.002e^{i0.6} & 0.004e^{i1.3} & 0.0001e^{-i3.0} & -0.0011 \end{pmatrix}$	-0.0047 0.0007 0.004 1
Gy	$\begin{pmatrix} 0.5 & 0.0042e^{-i3.0} & 0.4999e^{i1.6} & 0.0014e^{i0.3} \\ 0.0042e^{i3.0} & 0.0011 & 0.0014e^{-i1.2} & 0.0001e^{-i3.1} \\ 0.4999e^{-i1.6} & 0.0014e^{i1.2} & 0.5 & 0.0042e^{i1.5} \\ 0.0014e^{-i0.3} & 0.0001e^{i3.1} & 0.0042e^{-i1.5} & -0.0011 \end{pmatrix}$	-0.0048 0.0005 0.0043 1

Table 26: **Choi matrix representation of the GST estimated gateset.** This table lists Choi representations of the estimated gates, and their eigenvalues. Unitary gates have a spectrum $(1, 0, 0 \dots)$, just like pure quantum states. Negative eigenvalues are non-physical, and may represent either statistical fluctuations or violations of the CPTP model used by GST.

A.3 Gauge optimization to the target gates:

The gauge is chosen to minimize the Frobenius distance between the estimate and the target gates, with 99% weight given to the gate parameters, 1% to the SPAM parameters.

Operator	Hilbert-Schmidt vector (Pauli basis)	Matrix
ρ_0	0.7071 0.0065 -0.0045 0.701	$\begin{pmatrix} 0.9957 & 0.0056e^{i0.6} \\ 0.0056e^{-i0.6} & 0.0043 \end{pmatrix}$
E_0	0.701 -0.0008 -0.0003 -0.7011	$\begin{pmatrix} -2 \times 10^{-5} & 0.0006e^{i2.8} \\ 0.0006e^{-i2.8} & 0.9914 \end{pmatrix}$

Table 27: **The GST estimate of the SPAM operations.** Compare to Table 1.

	E_0	E_{-1}
ρ_0	0.004272	0.995728

Table 28: **GST estimate of SPAM probabilities.** Computed by taking the dot products of vectors in Table 27.

Gate	Superoperator (Pauli basis)
G_i	$\begin{pmatrix} 1 & 0 & 0 & 0 \\ -4 \times 10^{-6} & 1 & -5 \times 10^{-5} & -4 \times 10^{-5} \\ -2 \times 10^{-5} & 0.0001 & 0.9999 & 3 \times 10^{-6} \\ 2 \times 10^{-5} & -3 \times 10^{-5} & -8 \times 10^{-8} & 1 \end{pmatrix}$
G_x	$\begin{pmatrix} 1 & 0 & 0 & 0 \\ -2 \times 10^{-5} & 0.9999 & -2 \times 10^{-5} & -8 \times 10^{-6} \\ 5 \times 10^{-5} & 2 \times 10^{-5} & 0.0001 & -0.9999 \\ 1 \times 10^{-5} & 2 \times 10^{-5} & 0.9999 & 0.0001 \end{pmatrix}$
G_y	$\begin{pmatrix} 1 & 0 & 0 & 0 \\ -4 \times 10^{-5} & 3 \times 10^{-5} & 6 \times 10^{-6} & 0.9999 \\ 8 \times 10^{-7} & 5 \times 10^{-6} & 1 & 1 \times 10^{-7} \\ -1 \times 10^{-5} & -0.9999 & -3 \times 10^{-5} & -8 \times 10^{-6} \end{pmatrix}$

Table 29: **The GST estimate of the logic gate operations.** Compare to Table 2.

Gate	Process Infidelity	$1/2$ -width Trace Distance	$1/2$ -width \diamond -Norm	Frobenius Distance
Gi	0.000041	0.000052	0.00006	0.000136
Gx	0.000054	0.000081	0.000098	0.000203
Gy	0.000069	0.000071	0.000087	0.000181

Gate	Error Generator
Gi	$\begin{pmatrix} 0 & 0 & 0 & 0 \\ -4 \times 10^{-6} & -5 \times 10^{-5} & -5 \times 10^{-5} & -4 \times 10^{-5} \\ -2 \times 10^{-5} & 0.0001 & -0.0001 & 3 \times 10^{-6} \\ 2 \times 10^{-5} & -3 \times 10^{-5} & -8 \times 10^{-8} & -4 \times 10^{-5} \end{pmatrix}$
Gx	$\begin{pmatrix} 0 & 0 & 0 & 0 \\ -2 \times 10^{-5} & -0.0001 & -2 \times 10^{-5} & -8 \times 10^{-6} \\ 1 \times 10^{-5} & 2 \times 10^{-5} & -0.0001 & 0.0001 \\ -5 \times 10^{-5} & -2 \times 10^{-5} & -0.0001 & -0.0001 \end{pmatrix}$
Gy	$\begin{pmatrix} 0 & 0 & 0 & 0 \\ 1 \times 10^{-5} & -0.0001 & 3 \times 10^{-5} & 8 \times 10^{-6} \\ 8 \times 10^{-7} & 5 \times 10^{-6} & -4 \times 10^{-5} & 1 \times 10^{-7} \\ -4 \times 10^{-5} & 3 \times 10^{-5} & 6 \times 10^{-6} & -0.0001 \end{pmatrix}$

Table 30: **Comparison of GST estimated gates to target gates.** This table presents, for each of the gates, three different measures of distance or discrepancy from the GST estimate to the ideal target operation. See text for more detail. The column labeled “Error Generator” gives the Lindbladian \mathcal{L} that describes *how* the gate is failing to match the target. This error generator is defined by the equation $\hat{G} = G_{\text{target}}e^{\mathcal{L}}$.

Gate	Eigenvalues	Fixed pt	Rotn. axis	Diag. decay	Off-diag. decay
Gi	1	1	0	0.000018	0.000073
	$0.9999e^{i0.0}$	0	0.4704		
	$0.9999e^{-i0.0}$	0	0.384		
	1	0	-0.7945		
Gx	$0.9999e^{i1.6}$	1	0	0.000056	0.00008
	$0.9999e^{-i1.6}$	0	-1		
	0.9999	2×10^{-5}	-2×10^{-6}		
	1	3×10^{-5}	-2×10^{-5}		
Gy	$0.9999e^{i1.6}$	1	0	0.000039	0.000118
	$0.9999e^{-i1.6}$	-2×10^{-5}	-1×10^{-5}		
	1	0	1		
	1	1×10^{-5}	-2×10^{-5}		

Gate	Angle	Angle between Rotation Axes		
		Gi	Gx	Gy
Gi	0.000014		—	—
Gx	0.499968	—		0.499997π
Gy	0.499996	—	0.499997π	

Table 31: **Eigen-decomposition of estimated gates.** Each estimated gate is described in terms of: (1) the eigenvalues of the superoperator; (2) the gate’s fixed point (as a vector in $\mathcal{B}(\mathcal{H})$, in the Pauli basis); (3) the axis around which it rotates, as a vector in $\mathcal{B}(\mathcal{H})$; (4) the angle of the rotation that it applies; (5) the decay rate along the axis of rotation (“diagonal decay”); and (6) the decay rate perpendicular to the axis of rotation (“off-diagonal decay”). “—” indicates that the decomposition failed or couldn’t be interpreted.

Gate	Process Infidelity	$\frac{1}{2}$ -width Trace Distance	Rotation Axis	Rotation Angle	Sanity ✓
Gi	0.000041	0.000045	0 -0.026 -0.0816 0.9963	0.000016 π	0.000001
Gx	0.000054	0.000056	0 1 -5×10^{-6} 1×10^{-5}	0.499968 π	0.000003
Gy	0.000069	0.00007	0 -5×10^{-6} 1 -7×10^{-6}	0.499996 π	0.000001

Table 32: Information pertaining to the closest unitary gate to each of the estimated gates.

Gate	Choi matrix (Pauli basis)	Eigenvalues
Gi	$\begin{pmatrix} 1 & 1 \times 10^{-6}e^{i2.5} & 5 \times 10^{-6}e^{-i0.5} & 3 \times 10^{-5}e^{-i1.4} \\ 1 \times 10^{-6}e^{-i2.5} & 2 \times 10^{-5} & 5 \times 10^{-6}e^{-i1.9} & 2 \times 10^{-5}e^{i2.9} \\ 5 \times 10^{-6}e^{i0.5} & 5 \times 10^{-6}e^{i1.9} & 1 \times 10^{-6} & 1 \times 10^{-6}e^{i2.2} \\ 3 \times 10^{-5}e^{i1.4} & 2 \times 10^{-5}e^{-i2.9} & 1 \times 10^{-6}e^{-i2.2} & 2 \times 10^{-5} \end{pmatrix}$	-3×10^{-6} 6×10^{-6} 4×10^{-5} 1
Gx	$\begin{pmatrix} 0.5 & 0.5e^{-i1.6} & 1 \times 10^{-5}e^{-i2.6} & 1 \times 10^{-5}e^{-i1.3} \\ 0.5e^{i1.6} & 0.4999 & 4 \times 10^{-6}e^{-i2.2} & 1 \times 10^{-5}e^{-i1.3} \\ 1 \times 10^{-5}e^{i2.6} & 4 \times 10^{-6}e^{i2.2} & 2 \times 10^{-5} & 4 \times 10^{-6}e^{i1.6} \\ 1 \times 10^{-5}e^{i1.3} & 1 \times 10^{-5}e^{i1.3} & 4 \times 10^{-6}e^{-i1.6} & 5 \times 10^{-6} \end{pmatrix}$	-2×10^{-7} 2×10^{-5} 4×10^{-5} 0.9999
Gy	$\begin{pmatrix} 0.5 & 1 \times 10^{-5}e^{i2.5} & 0.4999e^{i1.6} & 2 \times 10^{-6}e^{i3.0} \\ 1 \times 10^{-5}e^{-i2.5} & 2 \times 10^{-5} & 4 \times 10^{-6}e^{i2.4} & 2 \times 10^{-7}e^{-i2.0} \\ 0.4999e^{-i1.6} & 4 \times 10^{-6}e^{-i2.4} & 0.5 & 1 \times 10^{-5}e^{i0.9} \\ 2 \times 10^{-6}e^{-i3.0} & 2 \times 10^{-7}e^{i2.0} & 1 \times 10^{-5}e^{-i0.9} & -3 \times 10^{-8} \end{pmatrix}$	-1×10^{-6} 2×10^{-5} 0.0001 0.9999

Table 33: **Choi matrix representation of the GST estimated gateset.** This table lists Choi representations of the estimated gates, and their eigenvalues. Unitary gates have a spectrum $(1, 0, 0 \dots)$, just like pure quantum states. Negative eigenvalues are non-physical, and may represent either statistical fluctuations or violations of the CPTP model used by GST.

A.4 Gauge optimization to TP

The gauge is chosen to make the gateset as trace-preserving as possible. This is done by minimizing the sum of the squared euclidian distance between the first row of each estimated gate matrix and the vector $(1, 0, \dots, 0)$. The Frobenius distance between the estimate and the target gateset, weighted by 10^{-4} , is added to the aforementioned sum of distances to give the final objective function. Ideally, a perfectly TP gateset will be found and the Frobenius distance term causes the optimization to choose the gateset closest to the target gates that is also in TP. If a perfectly TP gateset cannot be gauge-optimized to, then the resulting gateset compromises between being TP and being close to the target gateset, with the intent that the TP penalty term dominates.

Operator	Hilbert-Schmidt vector (Pauli basis)	Matrix
ρ_0	0.7071	$\begin{pmatrix} 0.9961 & 0.004e^{i0.6} \\ 0.004e^{-i0.6} & 0.0039 \end{pmatrix}$
	0.0046	
	-0.0032	
	0.7016	
E_0	0.7023	$\begin{pmatrix} 0.0004 & 0.0004e^{i2.2} \\ 0.0004e^{-i2.2} & 0.9928 \end{pmatrix}$
	-0.0003	
	-0.0005	
	-0.7017	

Table 34: **The GST estimate of the SPAM operations.** Compare to Table 1.

	E_0	E_{-1}
ρ_0	0.004272	0.995728

Table 35: **GST estimate of SPAM probabilities.** Computed by taking the dot products of vectors in Table 34.

Gate	Superoperator (Pauli basis)
Gi	$\begin{pmatrix} 1 & 0 & 0 & 0 \\ -4 \times 10^{-6} & 1 & -5 \times 10^{-5} & -4 \times 10^{-5} \\ -2 \times 10^{-5} & 0.0001 & 0.9999 & 3 \times 10^{-6} \\ 2 \times 10^{-5} & -3 \times 10^{-5} & -1 \times 10^{-7} & 1 \end{pmatrix}$
Gx	$\begin{pmatrix} 1 & 0 & 0 & 0 \\ -2 \times 10^{-5} & 0.9999 & -0.0011 & 0.0011 \\ 0.003 & 0.0006 & 0.0005 & -0.9999 \\ 0.0007 & 0.0006 & 0.9999 & -0.0003 \end{pmatrix}$
Gy	$\begin{pmatrix} 1 & 0 & 0 & 0 \\ -0.0034 & 0.0005 & 0.0003 & 0.9999 \\ 1 \times 10^{-6} & -0.0007 & 1 & -0.0007 \\ 0.0002 & -0.9999 & -0.0003 & -0.0005 \end{pmatrix}$

Table 36: **The GST estimate of the logic gate operations.** Compare to Table 2.

Gate	Process Infidelity	$1/2$ -width Trace Distance	$1/2$ -width \diamond -Norm	Frobenius Distance
Gi	0.000041	0.000052	0.00006	0.000136
Gx	0.000054	0.001734	0.002039	0.003598
Gy	0.000069	0.001807	0.002035	0.003664

Gate	Error Generator
Gi	$\begin{pmatrix} 0 & 0 & 0 & 0 \\ -4 \times 10^{-6} & -5 \times 10^{-5} & -5 \times 10^{-5} & -4 \times 10^{-5} \\ -2 \times 10^{-5} & 0.0001 & -0.0001 & 3 \times 10^{-6} \\ 2 \times 10^{-5} & -3 \times 10^{-5} & -1 \times 10^{-7} & -4 \times 10^{-5} \end{pmatrix}$
Gx	$\begin{pmatrix} 0 & 0 & 0 & 0 \\ -2 \times 10^{-5} & -0.0001 & -0.0011 & 0.0011 \\ 0.0007 & 0.0006 & -0.0001 & -0.0003 \\ -0.003 & -0.0006 & -0.0005 & -0.0001 \end{pmatrix}$
Gy	$\begin{pmatrix} 0 & 0 & 0 & 0 \\ -0.0002 & -0.0001 & 0.0003 & 0.0005 \\ -2 \times 10^{-7} & -0.0007 & -4 \times 10^{-5} & -0.0007 \\ -0.0034 & 0.0005 & 0.0003 & -0.0001 \end{pmatrix}$

Table 37: **Comparison of GST estimated gates to target gates.** This table presents, for each of the gates, three different measures of distance or discrepancy from the GST estimate to the ideal target operation. See text for more detail. The column labeled “Error Generator” gives the Lindbladian \mathcal{L} that describes *how* the gate is failing to match the target. This error generator is defined by the equation $\hat{G} = G_{\text{target}}e^{\mathcal{L}}$.

Gate	Eigenvalues	Fixed pt	Rotn. axis	Diag. decay	Off-diag. decay
Gi	1	1	0	0.000018	0.000073
	$0.9999e^{i0.0}$	0	0.4712		
	$0.9999e^{-i0.0}$	0	0.3834		
	1	0	-0.7943		
Gx	$0.9999e^{i1.6}$	1	0	0.000056	0.00008
	$0.9999e^{-i1.6}$	-1×10^{-6}	1		
	0.9999	0.0011	7×10^{-6}		
	1	0.0018	0.0006		
Gy	$0.9999e^{i1.6}$	1	0	0.000039	0.000118
	$0.9999e^{-i1.6}$	-0.0016	-7×10^{-6}		
	1	5×10^{-7}	1		
	1	0.0018	-0.0003		

Gate	Angle	Angle between Rotation Axes		
		Gi	Gx	Gy
Gi	0.000014		—	—
Gx	0.499968	—		0.5π
Gy	0.499996	—	0.5π	

Table 38: **Eigen-decomposition of estimated gates.** Each estimated gate is described in terms of: (1) the eigenvalues of the superoperator; (2) the gate’s fixed point (as a vector in $\mathcal{B}(\mathcal{H})$, in the Pauli basis); (3) the axis around which it rotates, as a vector in $\mathcal{B}(\mathcal{H})$; (4) the angle of the rotation that it applies; (5) the decay rate along the axis of rotation (“diagonal decay”); and (6) the decay rate perpendicular to the axis of rotation (“off-diagonal decay”). “—” indicates that the decomposition failed or couldn’t be interpreted.

Gate	Process Infidelity	$^{1/2}$ -width Trace Distance	Rotation Axis	Rotation Angle	Sanity ✓
Gi	0.000041	0.000045	0 0.0274 0.0809 -0.9963	0.000016 π	0.000001
Gx	0.000054	0.001549	0 -1 4×10^{-6} -0.0009	0.499968 π	0.010788
Gy	0.000069	0.001746	0 4×10^{-6} -1 0.0005	0.499996 π	0.010862

Table 39: Information pertaining to the closest unitary gate to each of the estimated gates.

Gate	Choi matrix (Pauli basis)	Eigenvalues
Gi	$\begin{pmatrix} 1 & 1 \times 10^{-6}e^{i2.5} & 5 \times 10^{-6}e^{-i0.5} & 3 \times 10^{-5}e^{-i1.4} \\ 1 \times 10^{-6}e^{-i2.5} & 2 \times 10^{-5} & 5 \times 10^{-6}e^{-i1.9} & 2 \times 10^{-5}e^{i2.9} \\ 5 \times 10^{-6}e^{i0.5} & 5 \times 10^{-6}e^{i1.9} & 1 \times 10^{-6} & 1 \times 10^{-6}e^{i2.2} \\ 3 \times 10^{-5}e^{i1.4} & 2 \times 10^{-5}e^{-i2.9} & 1 \times 10^{-6}e^{-i2.2} & 2 \times 10^{-5} \end{pmatrix}$	-3×10^{-6} 6×10^{-6} 4×10^{-5} 1
Gx	$\begin{pmatrix} 0.5 & 0.5e^{-i1.6} & 0.0007e^{i3.0} & 0.0005e^{-i1.2} \\ 0.5e^{i1.6} & 0.4999 & 0.0002e^{-i1.0} & 0.0009e^{-i1.0} \\ 0.0007e^{-i3.0} & 0.0002e^{i1.0} & 0.0002 & 7 \times 10^{-6}e^{i2.4} \\ 0.0005e^{i1.2} & 0.0009e^{i1.0} & 7 \times 10^{-6}e^{-i2.4} & -0.0002 \end{pmatrix}$	-0.0008 0.0001 0.0008 0.9999
Gy	$\begin{pmatrix} 0.5 & 0.0009e^{-i3.0} & 0.4999e^{i1.6} & 0.0002e^{i1.4} \\ 0.0009e^{i3.0} & 0.0003 & 0.0001e^{-i0.4} & 8 \times 10^{-6}e^{-i3.1} \\ 0.4999e^{-i1.6} & 0.0001e^{i0.4} & 0.5 & 0.0009e^{i1.3} \\ 0.0002e^{-i1.4} & 8 \times 10^{-6}e^{i3.1} & 0.0009e^{-i1.3} & -0.0002 \end{pmatrix}$	-0.0009 2×10^{-5} 0.0009 0.9999

Table 40: **Choi matrix representation of the GST estimated gateset.** This table lists Choi representations of the estimated gates, and their eigenvalues. Unitary gates have a spectrum $(1, 0, 0 \dots)$, just like pure quantum states. Negative eigenvalues are non-physical, and may represent either statistical fluctuations or violations of the CPTP model used by GST.

A.5 Gauge optimization to CPTP

The gauge is chosen to minimize a quantity indicating the “non-CPTP-ness” of the gateset, along with a slight preference for being close to the target gateset. In particular, we first optimize the gateset to TP (as described above), and then minimize the logarithm of a CP “penalty term” which we take as the sum of

1. the absolute values of any negative eigenvalues possessed by a gate’s Choi matrix
2. the absolute value of any negative eigenvalues of a state preparation density matrix
3. the absolute difference between the trace of a state preparation density matrix and one
4. the distance between an eigenvalue of an effect operator and the interval $[0, 1]$.

within the space of TP-preserving gauge transformations. This CP penalty term is added to the Frobenius distance between the estimate and the target gateset, weighted by 10^{-4} to give the final objective function.

Operator	Hilbert-Schmidt vector (Pauli basis)	Matrix
ρ_0	0.7071 0.0066 −0.0045 0.7011	$\begin{pmatrix} 0.9957 & 0.0056e^{i0.6} \\ 0.0056e^{-i0.6} & 0.0043 \end{pmatrix}$
E_0	0.701 −0.0008 −0.0003 −0.701	$\begin{pmatrix} 5 \times 10^{-5} & 0.0006e^{i2.8} \\ 0.0006e^{-i2.8} & 0.9914 \end{pmatrix}$

Table 41: **The GST estimate of the SPAM operations.** Compare to Table 1.

	E_0	E_{-1}
ρ_0	0.004272	0.995728

Table 42: **GST estimate of SPAM probabilities.** Computed by taking the dot products of vectors in Table 41.

Gate	Superoperator (Pauli basis)
G_i	$\begin{pmatrix} 1 & 0 & 0 & 0 \\ -4 \times 10^{-6} & 1 & -5 \times 10^{-5} & -4 \times 10^{-5} \\ -2 \times 10^{-5} & 0.0001 & 0.9999 & 3 \times 10^{-6} \\ 2 \times 10^{-5} & -3 \times 10^{-5} & -8 \times 10^{-8} & 1 \end{pmatrix}$
G_x	$\begin{pmatrix} 1 & 0 & 0 & 0 \\ -2 \times 10^{-5} & 0.9999 & 2 \times 10^{-5} & -2 \times 10^{-5} \\ 3 \times 10^{-5} & 1 \times 10^{-5} & 0.0001 & -0.9999 \\ 2 \times 10^{-5} & 3 \times 10^{-5} & 0.9999 & 0.0001 \end{pmatrix}$
G_y	$\begin{pmatrix} 1 & 0 & 0 & 0 \\ 1 \times 10^{-5} & 8 \times 10^{-6} & -2 \times 10^{-6} & 0.9999 \\ 8 \times 10^{-7} & 4 \times 10^{-5} & 1 & 1 \times 10^{-5} \\ 4 \times 10^{-5} & -0.9999 & -4 \times 10^{-5} & 2 \times 10^{-5} \end{pmatrix}$

Table 43: **The GST estimate of the logic gate operations.** Compare to Table 2.

Gate	Process Infidelity	$1/2$ -width Trace Distance	$1/2$ -width \diamond -Norm	Frobenius Distance
Gi	0.000041	0.000052	0.00006	0.000136
Gx	0.000054	0.00008	0.000095	0.000201
Gy	0.000069	0.00007	0.00008	0.000185

Gate	Error Generator
Gi	$\begin{pmatrix} 0 & 0 & 0 & 0 \\ -4 \times 10^{-6} & -5 \times 10^{-5} & -5 \times 10^{-5} & -4 \times 10^{-5} \\ -2 \times 10^{-5} & 0.0001 & -0.0001 & 3 \times 10^{-6} \\ 2 \times 10^{-5} & -3 \times 10^{-5} & -8 \times 10^{-8} & -4 \times 10^{-5} \end{pmatrix}$
Gx	$\begin{pmatrix} 0 & 0 & 0 & 0 \\ -2 \times 10^{-5} & -0.0001 & 2 \times 10^{-5} & -2 \times 10^{-5} \\ 2 \times 10^{-5} & 3 \times 10^{-5} & -0.0001 & 0.0001 \\ -3 \times 10^{-5} & -1 \times 10^{-5} & -0.0001 & -0.0001 \end{pmatrix}$
Gy	$\begin{pmatrix} 0 & 0 & 0 & 0 \\ -4 \times 10^{-5} & -0.0001 & 4 \times 10^{-5} & -2 \times 10^{-5} \\ 8 \times 10^{-7} & 4 \times 10^{-5} & -4 \times 10^{-5} & 1 \times 10^{-5} \\ 1 \times 10^{-5} & 8 \times 10^{-6} & -2 \times 10^{-6} & -0.0001 \end{pmatrix}$

Table 44: **Comparison of GST estimated gates to target gates.** This table presents, for each of the gates, three different measures of distance or discrepancy from the GST estimate to the ideal target operation. See text for more detail. The column labeled “Error Generator” gives the Lindbladian \mathcal{L} that describes *how* the gate is failing to match the target. This error generator is defined by the equation $\hat{G} = G_{\text{target}}e^{\mathcal{L}}$.

Gate	Eigenvalues	Fixed pt	Rotn. axis	Diag. decay	Off-diag. decay
Gi	1	1	0		
	$0.9999e^{i0.0}$	0	0.4704		
	$0.9999e^{-i0.0}$	0	0.384	0.000018	0.000073
	1	0	-0.7946		
Gx	$0.9999e^{i1.6}$	1	0		
	$0.9999e^{-i1.6}$	0	-1		
	0.9999	7×10^{-6}	6×10^{-6}	0.000056	0.00008
	1	3×10^{-5}	-2×10^{-5}		
Gy	$0.9999e^{i1.6}$	1	0		
	$0.9999e^{-i1.6}$	2×10^{-5}	-2×10^{-5}		
	1	0	1	0.000039	0.000118
	1	1×10^{-5}	-2×10^{-5}		

Gate	Angle	Angle between Rotation Axes		
		Gi	Gx	Gy
Gi	0.000014		—	—
Gx	0.499968	—		0.499991π
Gy	0.499996	—	0.499991π	

Table 45: **Eigen-decomposition of estimated gates.** Each estimated gate is described in terms of: (1) the eigenvalues of the superoperator; (2) the gate’s fixed point (as a vector in $\mathcal{B}(\mathcal{H})$, in the Pauli basis); (3) the axis around which it rotates, as a vector in $\mathcal{B}(\mathcal{H})$; (4) the angle of the rotation that it applies; (5) the decay rate along the axis of rotation (“diagonal decay”); and (6) the decay rate perpendicular to the axis of rotation (“off-diagonal decay”). “—” indicates that the decomposition failed or couldn’t be interpreted.

Gate	Process Infidelity	$^{1/2}$ -width Trace Distance	Rotation Axis	Rotation Angle	Sanity ✓
Gi	0.000041	0.000045	0 −0.026 −0.0816 0.9963	0.000016 π	0.000001
Gx	0.000054	0.000056	0 1 $−4 \times 10^{−6}$ $−5 \times 10^{−7}$	0.499968 π	0.000002
Gy	0.000069	0.00007	0 $−5 \times 10^{−6}$ 1 $3 \times 10^{−6}$	0.499996 π	0.000001

Table 46: Information pertaining to the closest unitary gate to each of the estimated gates.

Gate	Choi matrix (Pauli basis)	Eigenvalues
Gi	$\begin{pmatrix} 1 & 1 \times 10^{-6}e^{i2.5} & 5 \times 10^{-6}e^{-i0.5} & 3 \times 10^{-5}e^{-i1.4} \\ 1 \times 10^{-6}e^{-i2.5} & 2 \times 10^{-5} & 5 \times 10^{-6}e^{-i1.9} & 2 \times 10^{-5}e^{i2.9} \\ 5 \times 10^{-6}e^{i0.5} & 5 \times 10^{-6}e^{i1.9} & 1 \times 10^{-6} & 1 \times 10^{-6}e^{i2.2} \\ 3 \times 10^{-5}e^{i1.4} & 2 \times 10^{-5}e^{-i2.9} & 1 \times 10^{-6}e^{-i2.2} & 2 \times 10^{-5} \end{pmatrix}$	$−3 \times 10^{−6}$ $6 \times 10^{−6}$ $4 \times 10^{−5}$ 1
Gx	$\begin{pmatrix} 0.5 & 0.5e^{-i1.6} & 2 \times 10^{-5}e^{-i2.2} & 5 \times 10^{-6}e^{i0.2} \\ 0.5e^{i1.6} & 0.4999 & 1 \times 10^{-5}e^{-i2.6} & 9 \times 10^{-6}e^{-i1.5} \\ 2 \times 10^{-5}e^{i2.2} & 1 \times 10^{-5}e^{i2.6} & 1 \times 10^{-5} & 6 \times 10^{-6}e^{i2.4} \\ 5 \times 10^{-6}e^{-i0.2} & 9 \times 10^{-6}e^{i1.5} & 6 \times 10^{-6}e^{-i2.4} & 2 \times 10^{-5} \end{pmatrix}$	$1 \times 10^{−6}$ $1 \times 10^{−5}$ $4 \times 10^{−5}$ 0.9999
Gy	$\begin{pmatrix} 0.5 & 1 \times 10^{-5}e^{i1.4} & 0.4999e^{i1.6} & 1 \times 10^{-5}e^{-i0.8} \\ 1 \times 10^{-5}e^{-i1.4} & 8 \times 10^{-6} & 1 \times 10^{-5}e^{-i2.3} & 5 \times 10^{-6}e^{-i3.1} \\ 0.4999e^{-i1.6} & 1 \times 10^{-5}e^{i2.3} & 0.5 & 7 \times 10^{-6}e^{-i0.4} \\ 1 \times 10^{-5}e^{i0.8} & 5 \times 10^{-6}e^{i3.1} & 7 \times 10^{-6}e^{i0.4} & 1 \times 10^{-5} \end{pmatrix}$	$2 \times 10^{−9}$ $1 \times 10^{−5}$ 0.0001 0.9999

Table 47: **Choi matrix representation of the GST estimated gateset.** This table lists Choi representations of the estimated gates, and their eigenvalues. Unitary gates have a spectrum $(1, 0, 0 \dots)$, just like pure quantum states. Negative eigenvalues are non-physical, and may represent either statistical fluctuations or violations of the CPTP model used by GST.

B Pixel plots for intermediate gatesets

This appendix contains $2\Delta \log(\mathcal{L})$ pixel-plots for the intermediate estimates computed by GST on dataset “GSTBest_condensed” using a subset of the available data. Each estimate was computed using only base sequences of length up to L , for $L = 1, 2, 4, 8, \dots$. These plots are *not* identical to subsets of Figure 1, because the estimated gateset is different. Since these estimates only attempt to fit a subset of the data, they generally do much better at fitting that subset. (They do very badly, in general, at predicting longer sequences; for this reason the $2\Delta \log(\mathcal{L})$ values of those out-of-sample sequences are not shown). See main text and caption of Figure 1 for more details.

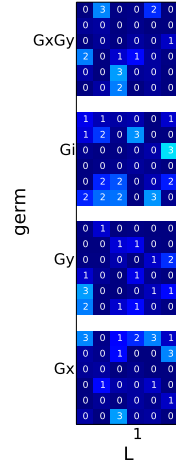


Figure 6: Box plot of iteration 0 ($L=1$) gateset $\log(\mathcal{L})$ values.

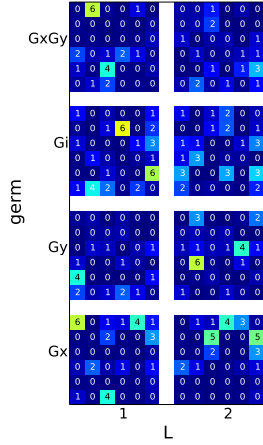


Figure 7: Box plot of iteration 1 ($L=2$) gateset $\log(\mathcal{L})$ values.

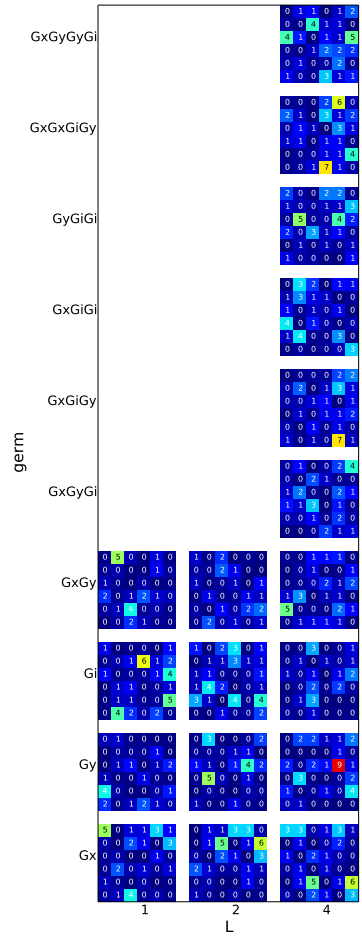


Figure 8: Box plot of iteration 2 ($L=4$) gateset $\log(\mathcal{L})$ values.

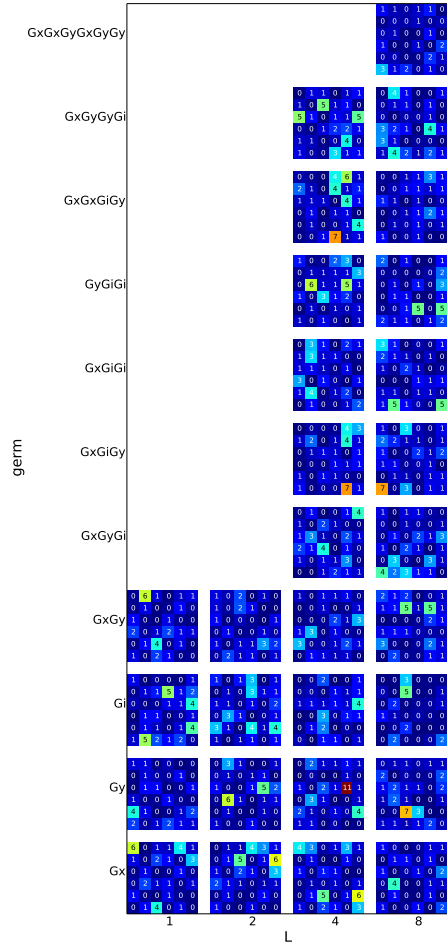


Figure 9: Box plot of iteration 3 ($L=8$) gateset $\log(\mathcal{L})$ values.

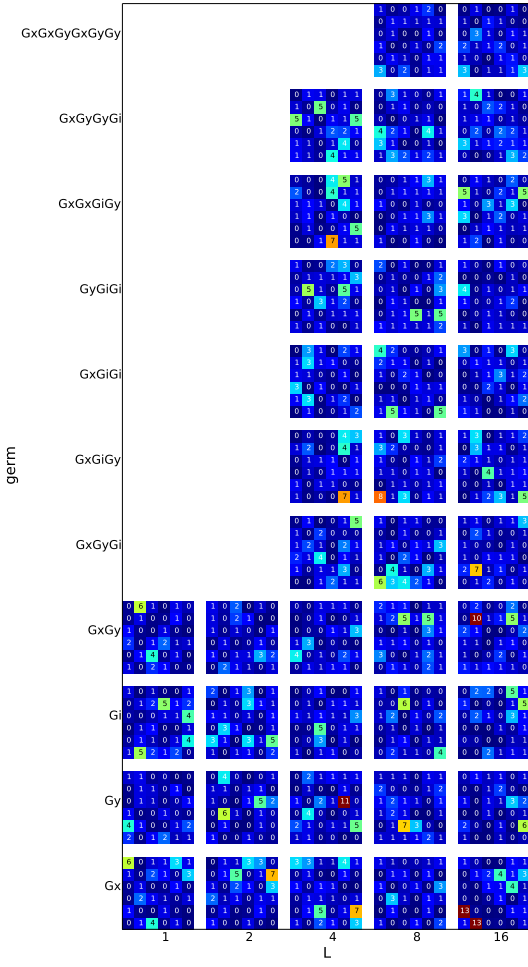


Figure 10: Box plot of iteration 4 ($L=16$) gateset $\log(\mathcal{L})$ values.

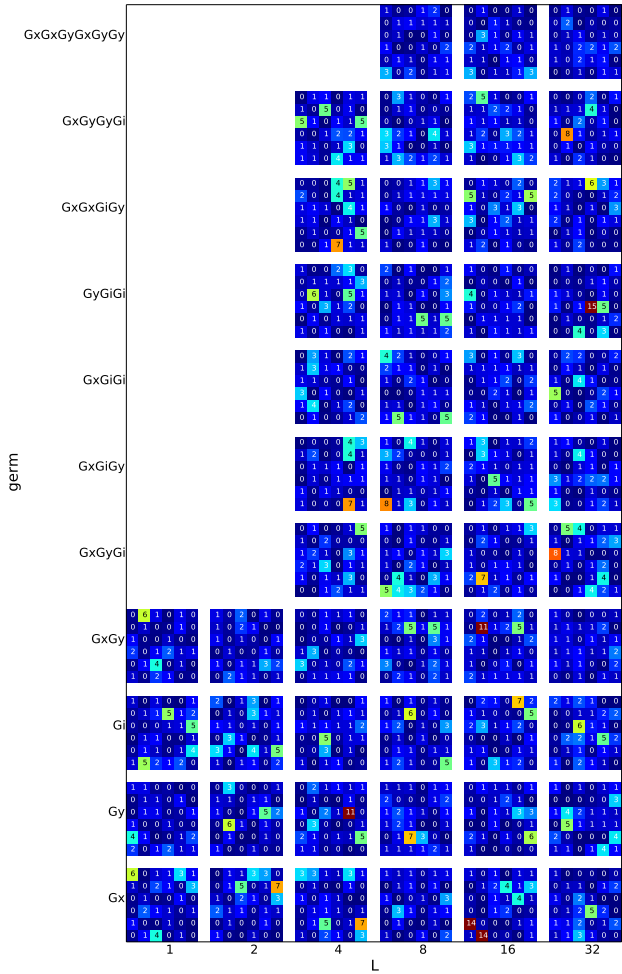


Figure 11: Box plot of iteration 5 ($L=32$) gateset $\log(\mathcal{L})$ values.

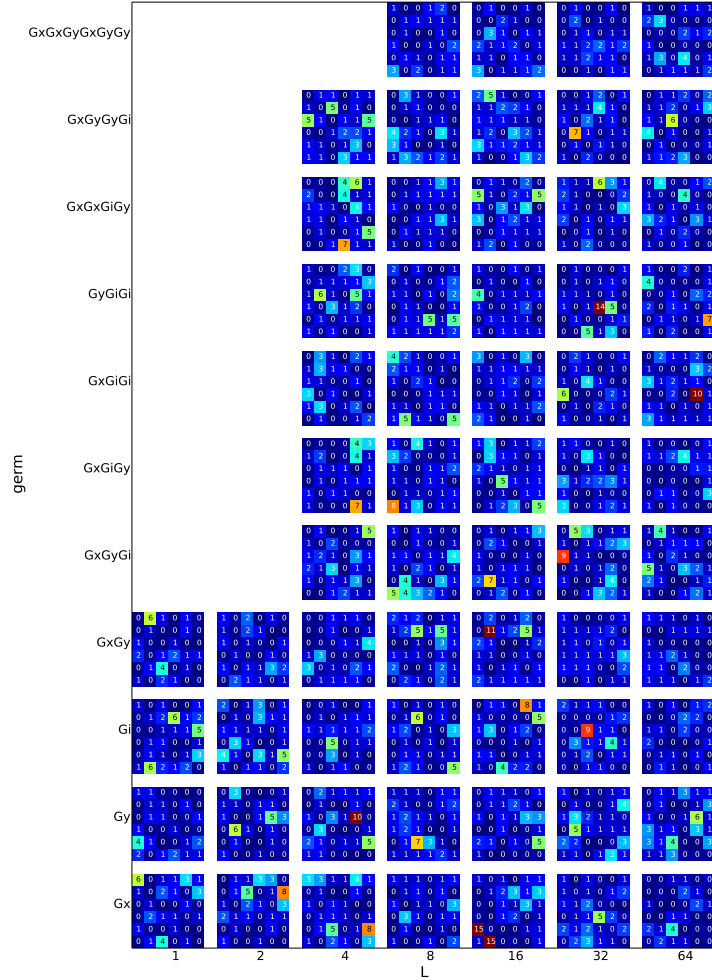


Figure 12: Box plot of iteration 6 ($L=64$) gateset $\log(\mathcal{L})$ values.

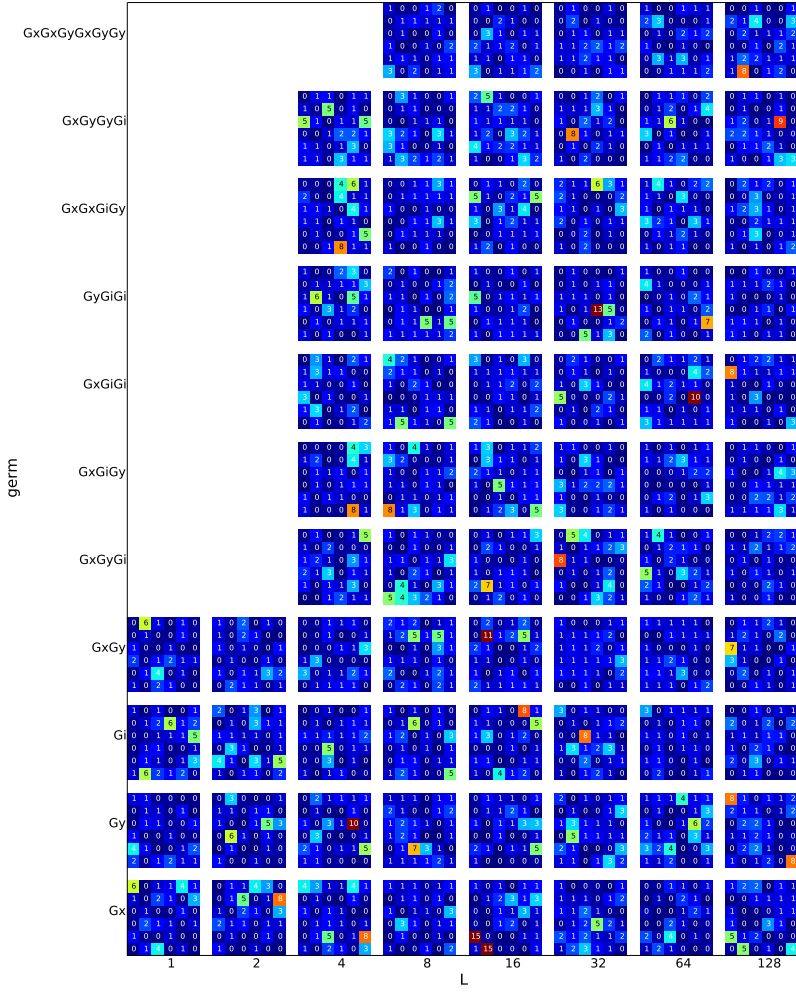


Figure 13: Box plot of iteration 7 ($L=128$) gateset $\log(\mathcal{L})$ values.

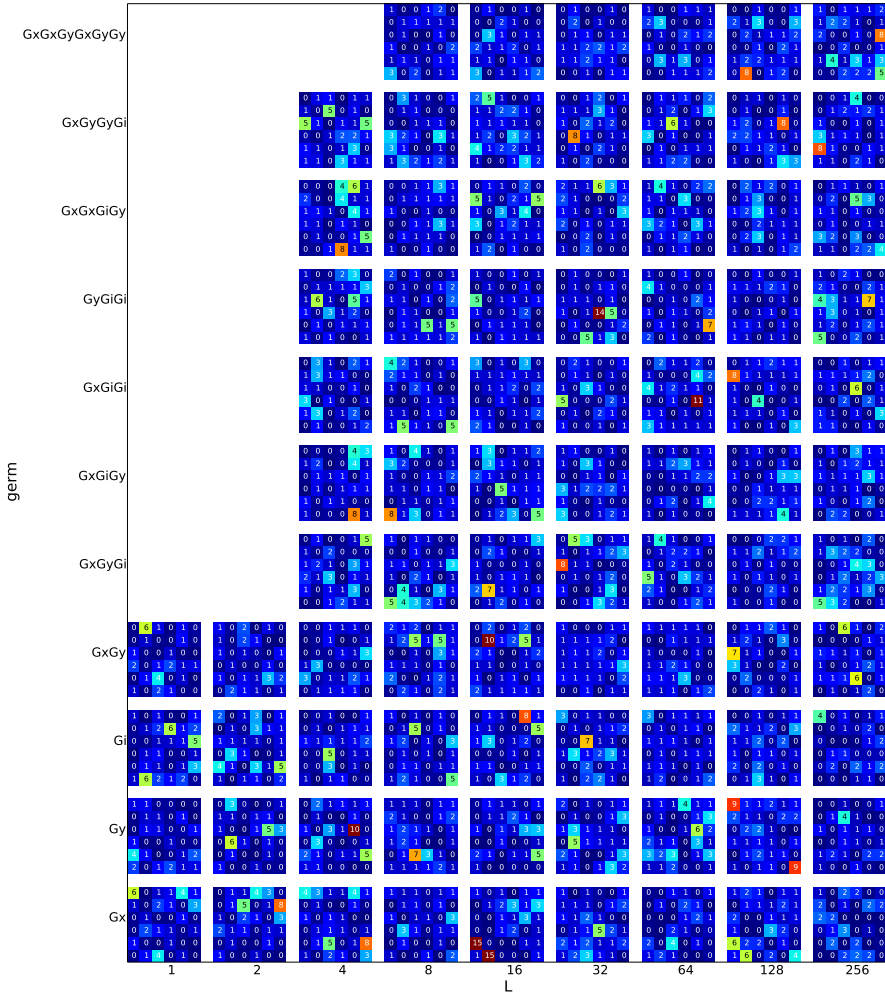


Figure 14: Box plot of iteration 8 ($L=256$) gateset $\log(\mathcal{L})$ values.

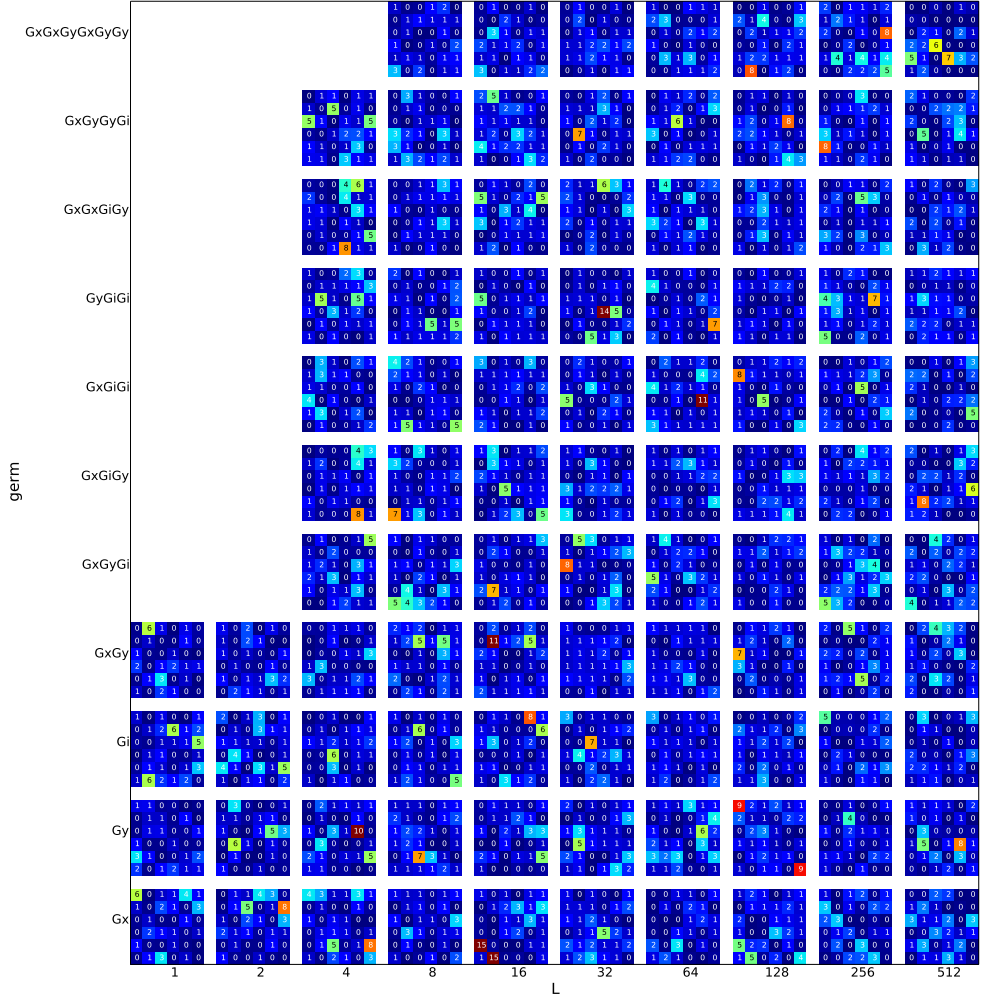


Figure 15: Box plot of iteration 9 ($L=512$) gateset $\log(\mathcal{L})$ values.

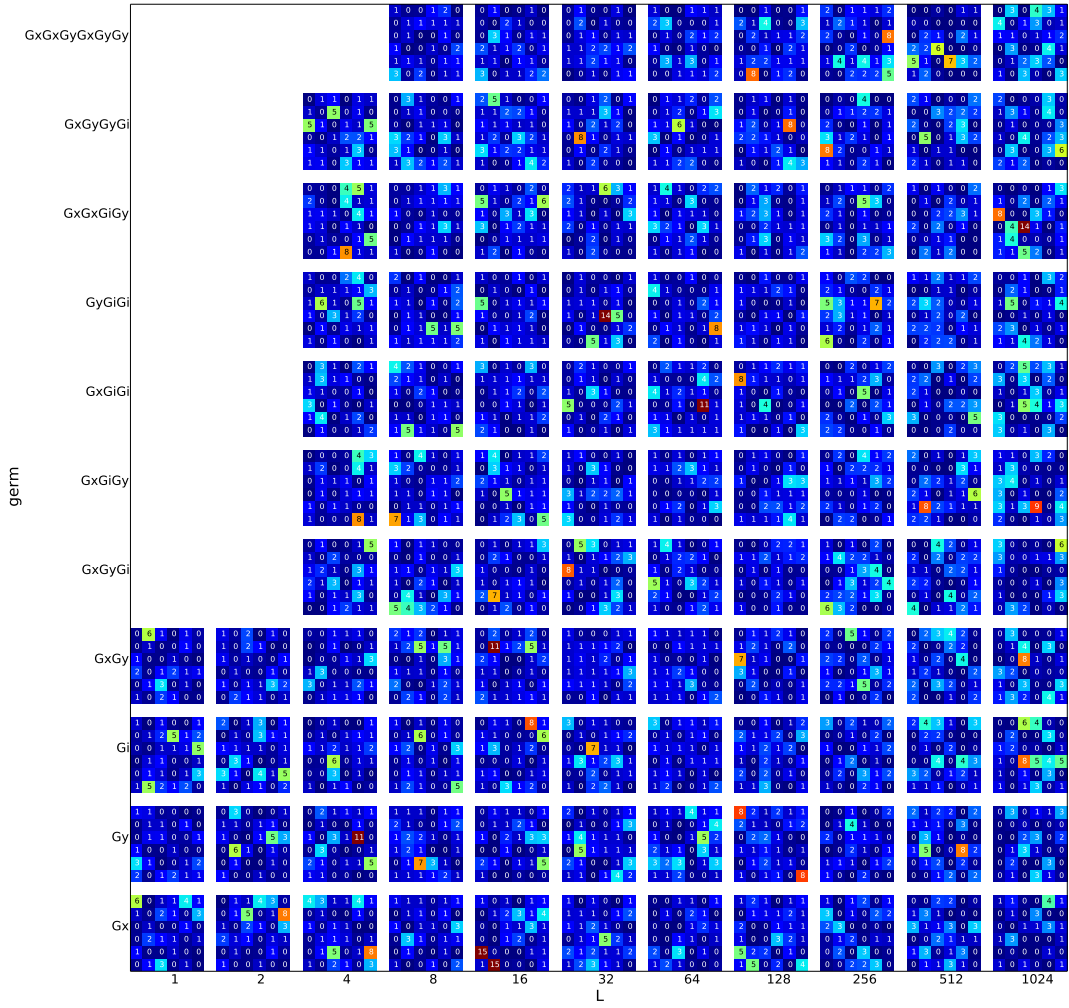


Figure 16: Box plot of iteration 10 ($L=1024$) gateset $\log(\mathcal{L})$ values.

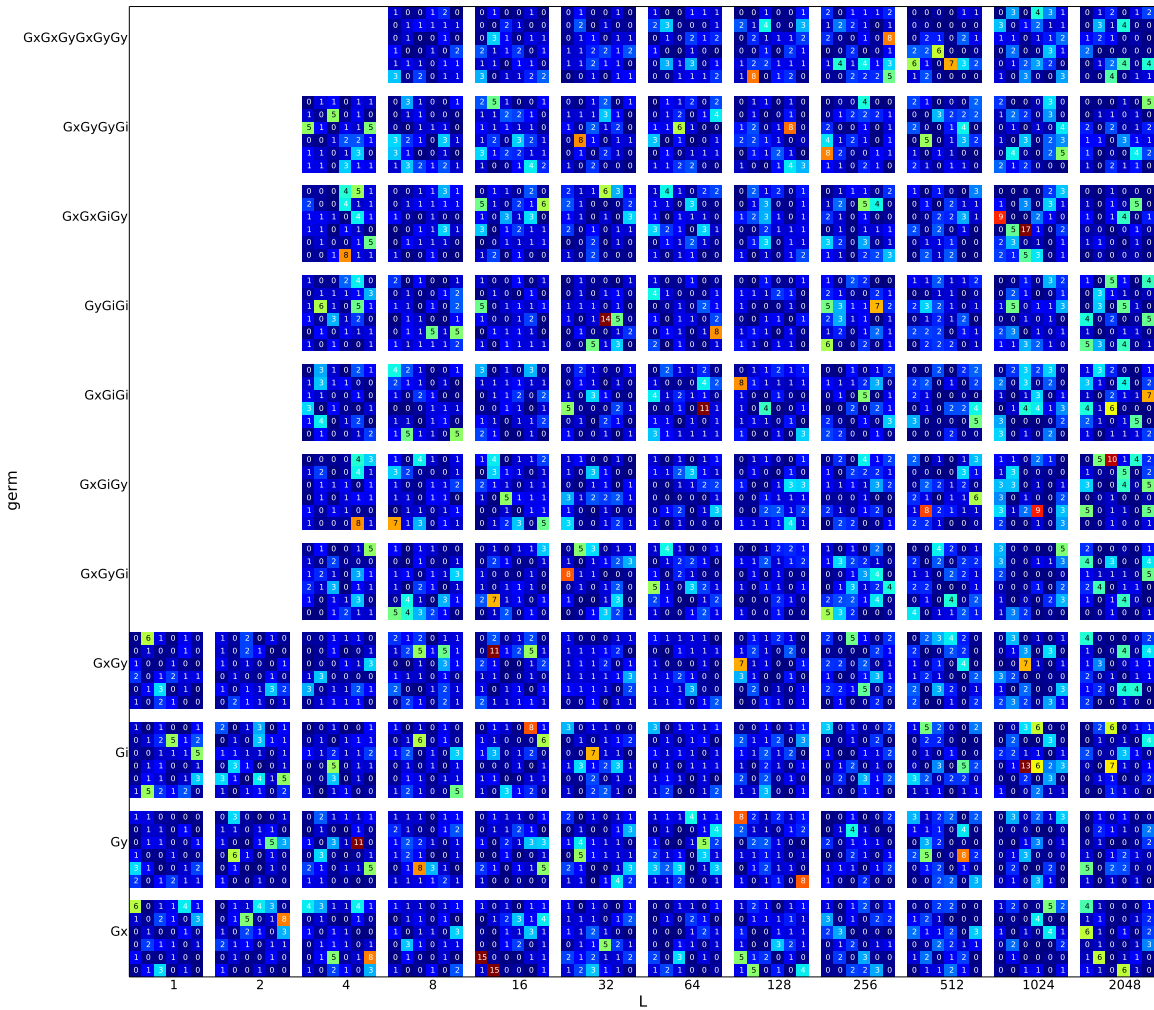


Figure 17: Box plot of iteration 11 ($L=2048$) gateset $\log(\mathcal{L})$ values.

C Whack-a-mole plots for select gate sequences

This appendix shows whimsically named “Whack-a-mole” plots. The point of these plots is to answer the question “Why is GST failing to fit the data in the block corresponding to base sequence XXX?” This question usually comes up after examining Figure 1 and identifying a particularly bad block. Usually, the answer is “Because GST was also trying to fit other data, in block YYY.” It’s often useful to know specifically *which* experiments are the stumbling block – i.e., which experiments would be even more badly fit by the estimate if we demanded that the data in base sequence XXX be fit better.

This question can be answered by examining the derivatives of $2\Delta \log(\mathcal{L})$ with respect to the gateset, evaluated at the stationary point (local minimum) corresponding to the GST estimate. By doing so, it is possible to simulate what would happen if, by demanding a better fit to the data in block XXX, we attempted to “whack” the large $2\Delta \log(\mathcal{L})$ values in block XXX. Unsurprisingly, whacking the XXX mole causes another one to pop up somewhere else (the GST fit is a local minimum of $2\Delta \log(\mathcal{L})$, and hopefully a global one too, so there is no way to improve $2\Delta \log(\mathcal{L})$). Where this occurs can provide some insight into what is stopping GST from fitting the data better (and therefore into what’s wrong with the gates).

In the Whack-a-mole plots shown below, each of the longest base sequences is independently “whacked” – i.e., the analysis attempts to reduce the $2\Delta \log(\mathcal{L})$ for that particular base sequence. The plots answer the question, “If the $2\Delta \log(\mathcal{L})$ contribution for this base sequence was forced downward by 10 units, how much would the $2\Delta \log(\mathcal{L})$ contributions for other experiments have to rise?” Thus, the number on the “whacked” block is always -10 . Blocks with negative values in this analysis are correlated tightly with the whacked block (improving the fit on the whacked block improves their fit as well). Blocks with large positive values are incompatible with the whacked block (improving the fit on the whacked block makes the fit on such a block worse). These plots can thus be used to identify inconsistencies in the data.

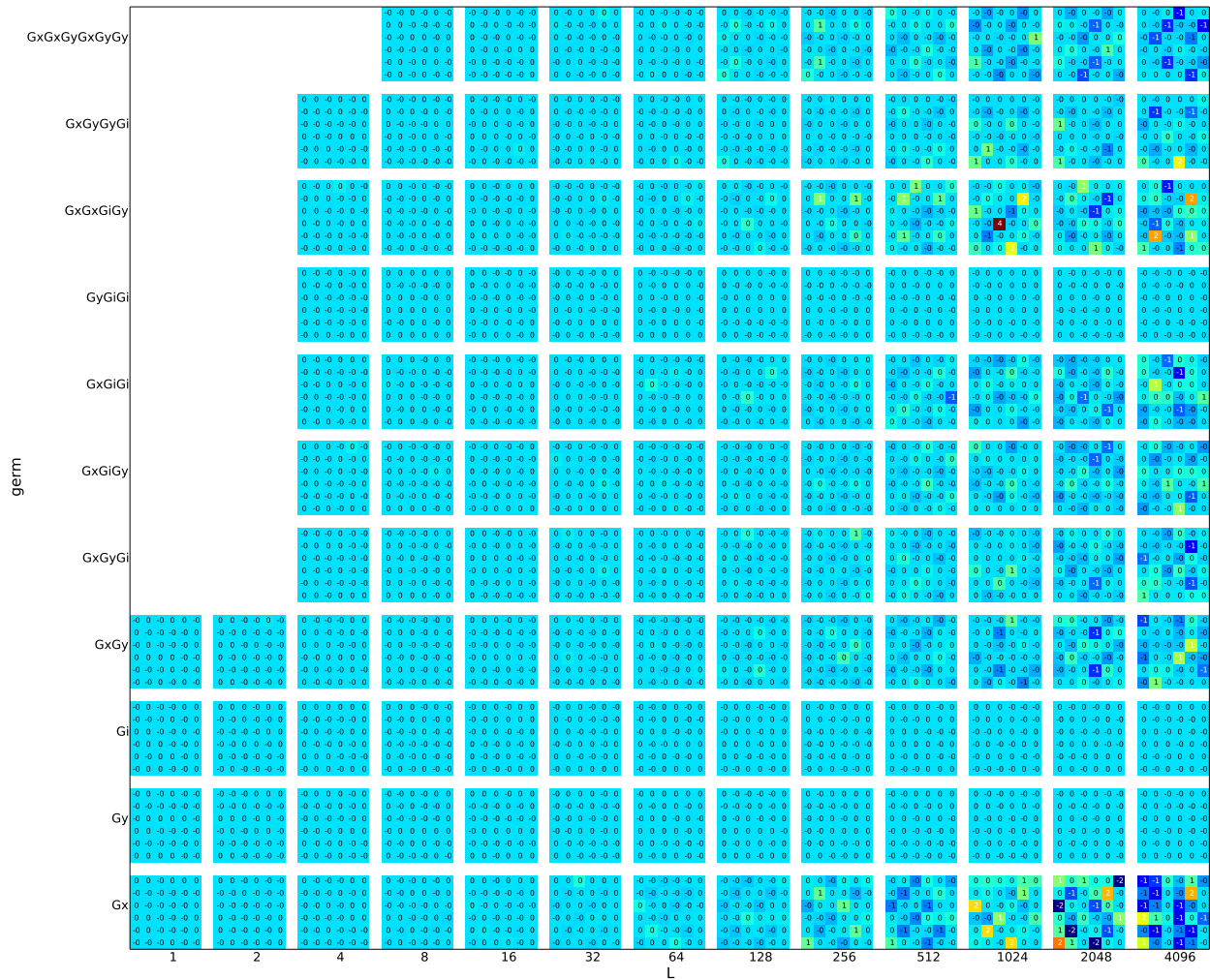


Figure 18: Whack-a-log(\mathcal{L})-mole box plot for Gx^{4096} . Hitting with hammer of weight 10.0.



Figure 19: Whack-a-log(\mathcal{L})-mole box plot for Gy^{4096} . Hitting with hammer of weight 10.0.

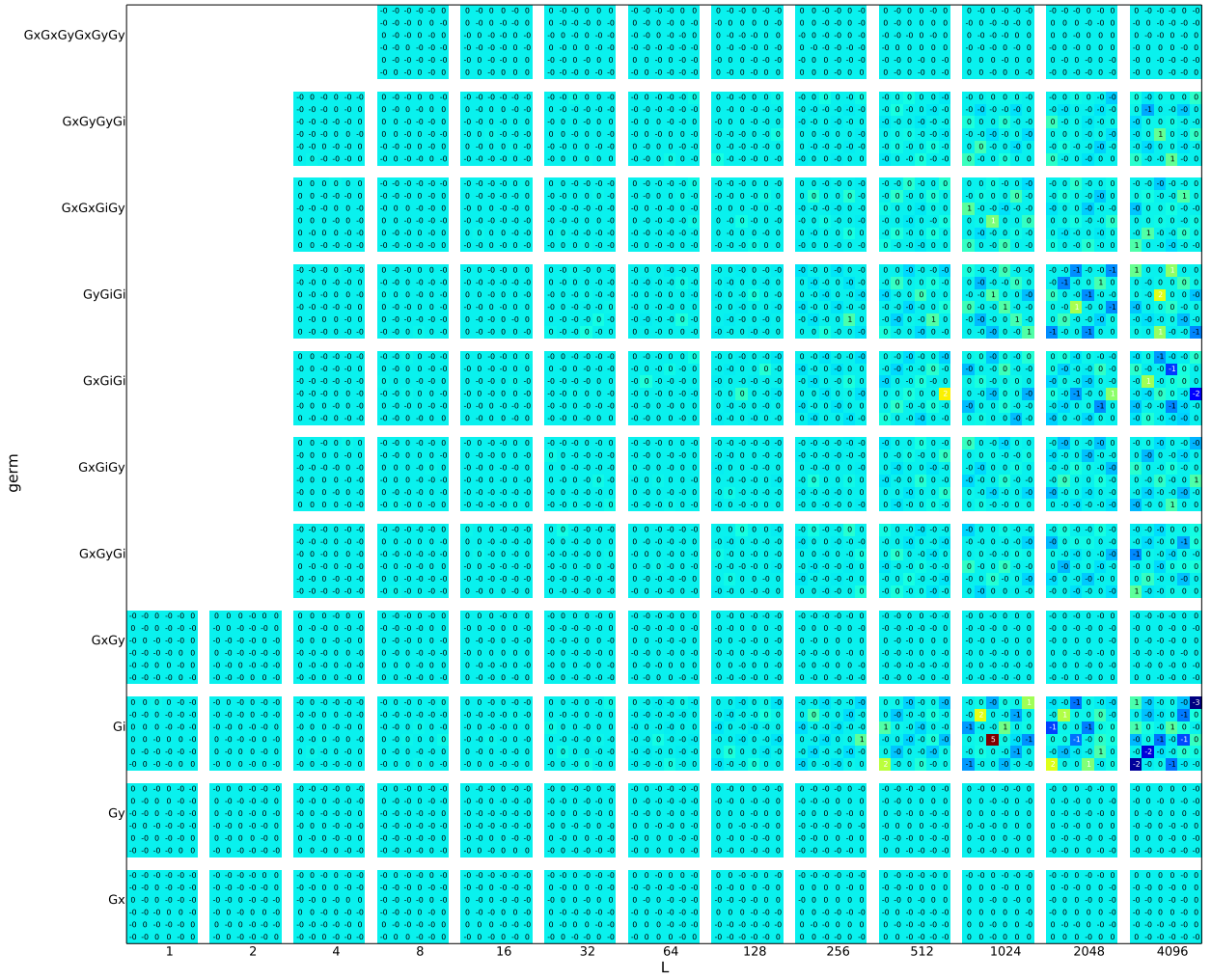


Figure 20: Whack-a-log(\mathcal{L})-mole box plot for Gi^{4096} . Hitting with hammer of weight 10.0.

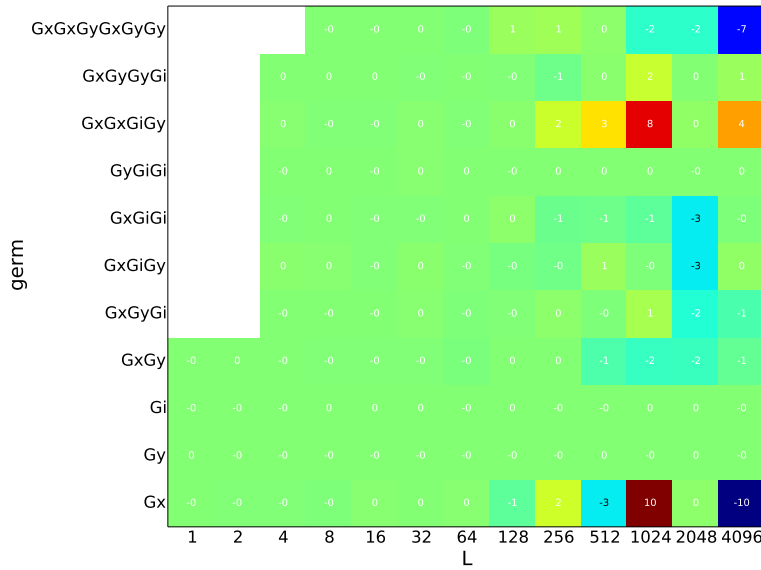


Figure 21: Whack-a-log(\mathcal{L})-mole box plot for Gx^{4096} , summed over fiducial matrix. Hitting with hammer of weight 10.0.

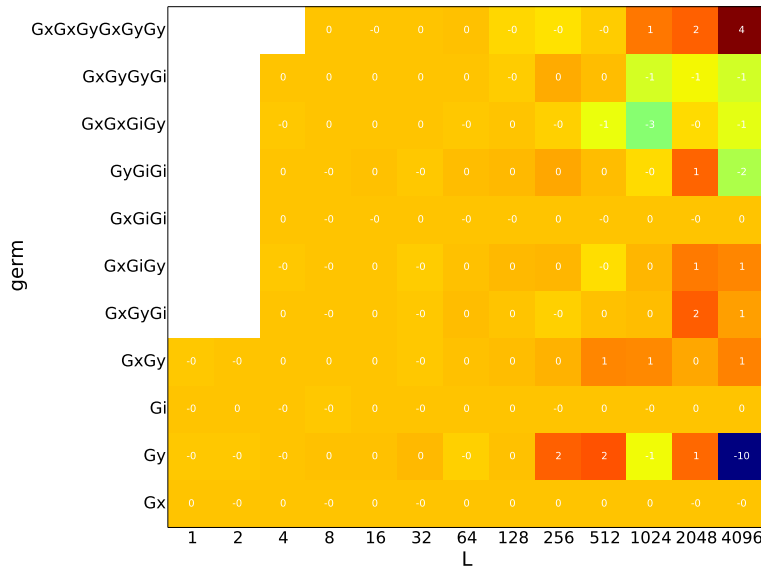


Figure 22: Whack-a-log(\mathcal{L})-mole box plot for Gy^{4096} , summed over fiducial matrix. Hitting with hammer of weight 10.0.

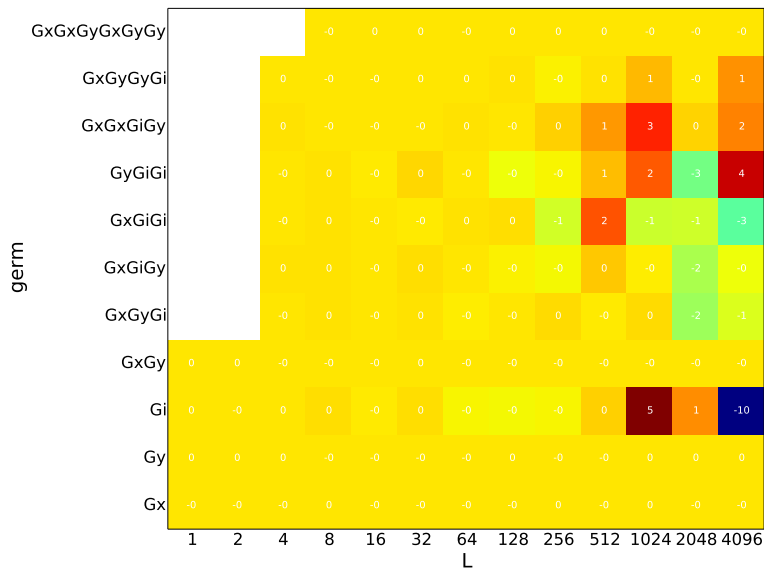


Figure 23: Whack-a-log(\mathcal{L})-mole box plot for Gi^{4096} , summed over fiducial matrix. Hitting with hammer of weight 10.0.